



**ICEBE**  
IMAGINEERING  
NATURE



## Diplomarbeit

# Solution Properties of Cellulose in Polar Solvents

ausgeführt zum Zwecke der Erlangung des akademischen Grades eines  
**Diplom-Ingenieurs (Dipl.-Ing.)**

unter der Leitung von

**Ao.Univ.Prof. Dipl.-Ing. Dr.techn. Michael Harasek**

(E166 Institut für Verfahrenstechnik, Umwelttechnik und Technische Biowissenschaften, TU Wien, Austria)

**Univ.Prof. Dr. Isao Wataoka**

(Institute for Biobased Material Science, Kyoto Institute of Technology, Japan)

eingereicht an der Technischen Universität Wien

Fakultät für Technische Chemie

von

**Sabine Ott, BSc**

Matr.Nr.: 01326095

Leystraße 108/2/7, 1200 Wien

Wien, am 05.02.2025

---

Sabine Ott



Die approbierte gedruckte Originalversion dieser Diplomarbeit ist an der TU Wien Bibliothek verfügbar  
The approved original version of this thesis is available in print at TU Wien Bibliothek.



**ICEBE**  
IMAGINEERING  
NATURE

Ich habe zur Kenntnis genommen, dass ich zur Drucklegung meiner Arbeit unter der Bezeichnung

## **Diplomarbeit**

nur mit Bewilligung der Prüfungskommission berechtigt bin.

Ich erkläre weiters Eides statt, dass ich meine Diplomarbeit nach den anerkannten Grundsätzen für wissenschaftliche Abhandlungen selbstständig ausgeführt habe und alle verwendeten Hilfsmittel, insbesondere die zugrunde gelegte Literatur, genannt habe.

Weiters erkläre ich, dass ich dieses Diplomarbeitsthema bisher weder im In- noch Ausland (einer Beurteilerin/einem Beurteiler zur Begutachtung) in irgendeiner Form als Prüfungsarbeit vorgelegt habe und dass diese Arbeit mit der vom Begutachter beurteilten Arbeit übereinstimmt.

Wien, am 05.02.2025

---

Sabine Ott



Die approbierte gedruckte Originalversion dieser Diplomarbeit ist an der TU Wien Bibliothek verfügbar  
The approved original version of this thesis is available in print at TU Wien Bibliothek.

# Acknowledgments

At this point, I want to thank all the people who supported me during this thesis. I want to thank my professor and supervisor from TU Wien, Vienna, Mr. Michael Harasek for accepting my wish to pursue my thesis overseas in Japan and supporting me throughout the way. I also want to thank my supervisor from Kyoto Institute of Technology, Japan, Mr. Isao Wataoka for accepting me as an exchange student into his laboratory and making this work possible.

A thousand thanks to Ms. Cornelia Hofbauer, Mr. Sebastian Serna Loaiza, and my family for their strong and unwavering support and their open ears from home.

At last, I want to mention a very special person to me and a million thanks to Ms. Cornelia Hofbauer, my best friend for over 15 years, for supporting me throughout this, not only fun times in Japan, like the most incredible person.

Thank you!



Die approbierte gedruckte Originalversion dieser Diplomarbeit ist an der TU Wien Bibliothek verfügbar  
The approved original version of this thesis is available in print at TU Wien Bibliothek.

## Abstract

Microcrystalline cellulose (MCC) is one of the most researched materials in the last decade and will become even more utilized in the future as a sustainable material extracted from wood or celluloses from annual plants [18]. Typically, MCCs are used in their insoluble form because of their properties as an inert substance, insoluble filler, or bulking agent in many oral medications and supplements [50]. However, there are scenarios where MCC can be modified or chemically treated to make it soluble or partially soluble and be used for various applications such as pharmaceutical coatings, cosmetics, and films [27]. As of now, the chemicals that are used to solubilize cellulose, e.g. alkali or acetic acids, can be environmentally problematic and pose disposal and wastewater treatment challenges [40]. To become more environmentally friendly and sustainable, one of the promising ways to leave toxic solvents behind are ionic liquids (IL) because of their non-volatility and high capability of solving cellulose [27], extremely low vapor pressure, high ionic conductivity, thermal stability [20], and potential recyclability [29]. These unique characteristics make them especially relevant for future biorefinery and biomass pretreatment applications [27] as “green” solvents [51]. Their ability to dissolve cellulose is driven by the ability of the IL anions to preferentially hydrogen bond to cellulose and solubilize the biopolymer through a no-derivatizing process. Correspondingly, the hydrogen bond accepting ability of the ionic liquid anion is largely attributed to the successful dissolution of cellulose in an IL. Select studies also show that the IL cation plays an ancillary role in the dissolution process through interactions with oxygen atoms on the hydroxyl groups of cellulose [36]. One of the most researched ILs is imidazolium-based [27], such as 1-ethyl-3-methylimidazolium acetate (EmimAc). In addition, IL can be designed for specific processes by altering the cation and anion structures and a new class of choline- and amino acid-based IL have emerged, such as Choline Chloride-Urea (ChCl-Urea) IL, Choline Chloride-Glycerol (ChCl-Glycerol) and L-Proline-based IL [6, 34], fulfilling the need to be biodegradable, non-toxic, and safe for producing biocompatible compounds [29]. Therefore they have been suggested as a replacement for volatile organic compounds (VOCs) in industrial separation processes and application in chemical synthesis, electrochemistry, and nanotechnology [30].

To make IL usable for industrial utilization in cellulose processing is, besides recycling, the understanding of cellulose behavior during the solution process in the presence of not only the IL, but also the “co-solvents”, that are in fact non-solvents, such as dimethyl sulfoxide (DMSO)

[27]. Those co-solvents are needed to e.g. reduce viscosity, fine-tune the properties, and reduce the overall cost of the solvent system [34].

Solvents that donate hydrogen bonds, such as water and alcohol, tend to associate with negatively charged anions found in IL. When these solvents are mixed with ILs, they compete with the IL anions for interactions, which can interfere with the ability of the ILs to dissolve cellulose. This preferential binding between protic solvents and IL anions ultimately leads to the precipitation of cellulose from IL-protic solvent mixtures. However, some organic solvents can function as co-solvents under certain conditions and temperatures. Polar aprotic solvents like DMSO, dimethylformamide (DMF), and 1,3-dimethyl-2-imidazolidinone (DMI) can be used as co-solvents for cellulose when mixed with ILs, despite having little cellulose dissolving capacity on their own [36].

Once cellulose is dissolved in a given solvent system, it is important to determine its molecular weight, as this is necessary for the design and application of cellulose-based materials [18, 45].

The development of effective methods that can be used to accurately measure the molecular weight parameters of cellulose is not only urgently needed for the structural characterization of cellulose, but also forms the basis for understanding the relationship between the structure and properties of cellulose-based materials [54]. The viscosity method can be used to obtain the relative viscosity average molecular weight via the relationship between the intrinsic viscosity of cellulose solution and the molecular weight of cellulose. It has become the standard method used in cellulose industries owing to its simple instrumentation and convenient operation [33].

To be able to obtain this value without performing time-consuming measurements, the Mark-Houwink-Sakurada (MHS) formula is widely used [33] to calculate the molecular mass of polymers, if the constants  $a$  and  $K$  are known.

This thesis examines two separate topics, first, the molecular mass of Avicel® cellulose PH-101 can be calculated by solving it in an N, N-Dimethylacetamide (DMAc)/Lithium chloride (LiCl) mixture. The existing publication of McCormick *et. al* [7] is used as the base for the first aim, because it is one of the most researched solvent systems for solving cellulose and also a highly cited paper in terms of calculating molecular mass of cellulose. The second topic is to determine the intrinsic viscosity of Avicel in EmimAc, EmimAc-Water, and EmimAc-DMSO mixtures to compare the results among them.

## Abstract (German)

Mikrokristalline Cellulose (MCC) ist eines der am meisten erforschten Materialien des letzten Jahrzehnts und wird in Zukunft noch stärker genutzt werden, da es sich um ein nachhaltiges Material handelt, das aus Holz oder Cellulosen von einjährigen Pflanzen gewonnen wird [13]. Typischerweise wird MCC in seiner unlöslichen Form verwendet, da es aufgrund seiner Eigenschaften als inerte Substanz, unlöslicher Füllstoff oder Volumen- bzw. Verdickungsmittel in vielen oralen Medikamenten und Nahrungsergänzungsmitteln genutzt werden kann [42]. Es gibt jedoch Szenarien, in denen MCC modifiziert oder chemisch behandelt werden kann, um es löslich oder teilweise löslich zu machen und für verschiedene Anwendungen wie pharmazeutische Beschichtungen, Kosmetika und Filme verwendet zu werden [22]. Bis jetzt sind die Chemikalien, die verwendet werden, um Cellulose löslich zu machen, z.B. Alkalien oder Essigsäuren, umweltproblematisch und stellen Herausforderungen bei der Entsorgung und Abwasserbehandlung dar [32]. Um umweltfreundlicher und nachhaltiger zu werden, gehören Ionenflüssigkeiten (IL) zu den vielversprechenden Mitteln, um toxische Lösungsmittel zu vermeiden, aufgrund ihrer Nicht-Flüchtigkeit und hohen Fähigkeit, Cellulose zu lösen [22], extrem niedrigen Dampfdruck, hoher ionischer Leitfähigkeit, thermischer Stabilität [15] und möglicher Rezyklierbarkeit [24]. Diese einzigartigen Eigenschaften machen sie besonders relevant für zukünftige Biorefinery- und Biomassevorbehandlungsanwendungen [22] als „grüne“ Lösungsmittel [43]. Ihre Fähigkeit, Cellulose zu lösen, wird durch die Fähigkeit der IL-Anionen bestimmt, bevorzugt Wasserstoffbrückenbindungen mit Cellulose zu bilden und das Biopolymer durch einen nicht derivatisierenden Prozess zu solubilisieren. Entsprechend wird die Fähigkeit des Anions der Ionenflüssigkeit, Wasserstoffbrücken aufzunehmen, weitgehend dem erfolgreichen Auflösen von Cellulose in einer IL zugeschrieben. Ausgewählte Studien zeigen auch, dass das IL-Kation eine unterstützende Rolle im Auflösungsprozess durch Wechselwirkungen mit Sauerstoffatomen an den Hydroxylgruppen der Cellulose spielt [29]. Eine der am meisten erforschten ILs ist die auf Imidazolium basierende [22], wie 1-Ethyl-3-methylimidazoliumacetat (EmimAc). Darüber hinaus können ILs für spezifische Prozesse durch Veränderung der Kationen- und Anionstrukturen entworfen werden, und eine neue Klasse von cholin- und aminoacid-basierten ILs ist entstanden, wie Cholinchlorid-Urea (ChCl-Urea)-IL, Cholinchlorid-Glycerin (ChCl-Glycerol) und L-Prolin-basierte ILs [5, 27], die die Notwendigkeit erfüllen, biologisch abbaubar, ungiftig und sicher für die Herstellung biokompatibler Verbindungen zu sein [24]. Daher wurden sie als Ersatz für flüchtige organische Verbindungen (VOCs) in industriellen

Trennprozessen und Anwendungen in der chemischen Synthese, Elektrochemie und Nanotechnologie vorgeschlagen [25].

Um ILs für die industrielle Nutzung in der Celluloseverarbeitung einsetzbar zu machen, ist neben dem Recycling das Verständnis des Verhaltens von Cellulose während des Lösungsvorgangs in Gegenwart nicht nur der IL, sondern auch der „Co-Lösungsmittel“, die in der Tat keine Lösungsmittel sind, wie Dimethylsulfoxid (DMSO) [22]. Diese Co-Lösungsmittel werden benötigt, um z.B. die Viskosität zu verringern, die Eigenschaften fein abzustimmen und die Gesamtkosten des Lösungsmittelsystems zu senken [27]. Lösungsmittel, die Wasserstoffbrückenbindungen spenden, wie Wasser und Alkohol, neigen dazu, mit negativ geladenen Anionen in ILs zu assoziieren. Wenn diese Lösungsmittel mit ILs gemischt werden, konkurrieren sie mit den IL-Anionen um Wechselwirkungen, was die Fähigkeit der ILs, Cellulose zu lösen, beeinträchtigen kann. Diese bevorzugte Bindung zwischen protischen Lösungsmitteln und IL-Anionen führt schließlich zur Ausfällung von Cellulose aus IL-protischen Lösungsmittelgemischen. Einige organische Lösungsmittel können jedoch unter bestimmten Bedingungen und Temperaturen als Co-Lösungsmittel wirken. Polare aprotische Lösungsmittel wie DMSO, Dimethylformamid (DMF) und 1,3-Dimethyl-2-imidazolidinon (DMI) können als Co-Lösungsmittel für Cellulose verwendet werden, wenn sie mit ILs gemischt werden, obwohl sie für sich allein eine geringe Fähigkeit zur Lösung von Cellulose haben [29].

Sobald Cellulose in einem bestimmten Lösungsmittelsystem gelöst ist, ist es wichtig, ihr Molekulargewicht zu bestimmen, da dies für das Design und die Anwendung von Cellulose-basierten Materialien notwendig ist [13, 36]. Die Entwicklung effektiver Methoden zur genauen Messung der Molekulargewichtparameter von Cellulose ist nicht nur dringend für die strukturelle Charakterisierung von Cellulose erforderlich, sondern bildet auch die Grundlage für das Verständnis der Beziehung zwischen Struktur und Eigenschaften von Cellulose-basierten Materialien [46]. Die Viskositätsmethode kann verwendet werden, um das relative Viskositätsdurchschnitts-Molekulargewicht über die Beziehung zwischen der intrinsischen Viskosität der Celluloselösung und dem Molekulargewicht der Cellulose zu ermitteln. Sie hat sich als Standardmethode in der Celluloseindustrie etabliert, da sie einfache Instrumentierung und eine bequeme Handhabung bietet [26].

Um diesen Wert zu ermitteln, ohne zeitaufwändige Messungen durchzuführen, wird die Mark-Houwink-Sakurada (MHS)-Formel häufig verwendet [26], um die Molekülmasse von Polymeren zu berechnen, wenn die Konstanten  $a$  und  $K$  bekannt sind.

Diese Arbeit untersucht zwei Themen. Zum einen, die Berechnung der Molekülmasse von Avicel<sup>®</sup> Cellulose PH-101, indem sie in einer N,N-Dimethylacetamid (DMAc)/Lithiumchlorid (LiCl)-Mischung gelöst wird. Die bestehende Veröffentlichung von McCormick et al. [6] wird als Basis für das erste Ziel verwendet, da es eines der am meisten erforschten Lösungsmittelsysteme für die Lösung von Cellulose ist und auch ein hochzitatierter Artikel zur Berechnung der Molekülmasse von Cellulose. Das zweite Thema ist die Bestimmung der intrinsischen Viskosität von Avicel in EmimAc, EmimAc-Wasser und EmimAc-DMSO Mischungen, um die erhaltenen Ergebnisse zu vergleichen.



Die approbierte gedruckte Originalversion dieser Diplomarbeit ist an der TU Wien Bibliothek verfügbar  
The approved original version of this thesis is available in print at TU Wien Bibliothek.

# Table of Contents

Table of Contents .....	1
Table of Figures.....	3
List of Tables .....	5
List of Abbreviations .....	6
1 INTRODUCTION .....	8
1.1 State of the art / research problem .....	8
1.2 Purpose of the thesis / scientific question.....	9
1.3 Scope of the thesis .....	10
2 THEORETICAL BACKGROUND .....	11
2.1 Cellulose .....	11
2.2 Soluble cellulose: Organic and inorganic solvents.....	13
3 MATERIALS AND METHODS .....	16
3.1 Used materials .....	16
3.2 Experimental setup / preparations .....	19
3.3 Viscosity .....	20
3.3.1 Measurement .....	22
3.4 Density.....	24
3.4.1 Measurement .....	25
4 RESULTS AND DISCUSSION – Molecular Weight of Avicel .....	26
4.1 Viscosity .....	26
4.2 Density result evaluation .....	27
4.3 Intrinsic viscosity result evaluation .....	29
4.4 Calculation of the molecular weight of Avicel.....	31
5 RESULTS AND DISCUSSION – Calculation and comparison of the intrinsic viscosities of MCC solved in EmimAc-solvent systems .....	33
5.1 Water content.....	33
5.2 Viscosity result evaluation .....	34
5.3 Density result evaluation .....	37
5.4 Intrinsic viscosity results evaluation .....	39
6 CONCLUSION .....	47

7	References .....	49
8	Appendix .....	55
8.1	Figures.....	55
8.2	Calculation of heat flux Q for water/air – viscosity measurement .....	57

## Table of Figures

Figure 2-1 A structural section of the origin of cellulose, showing the main components of microfibril. Taken from [21] .....	12
Figure 2-2 Schematic dissolution process of cellulose fibers. Taken from [14]. .....	15
Figure 3-1 Chemical structure of Avicel PH-101. Taken from [46] .....	16
Figure 3-2 Chemical structure of EmimAc [13].....	17
Figure 3-3 Schematic of a plot of $\eta_{sp}/c$ and $\ln(\eta_{rel})/c$ versus $c$ , and extrapolation to zero concentration to determine $[\eta]$ [48]. .....	23
Figure 3-4 Schematic Ubbelohde viscometer, A marks the line where the meniscus lies when the time measurement starts, and B marks the line where the time will be stopped [17] .....	24
Figure 4-1 Time for viscosity measurement of DMAc/LiCl at 25°C and at 30°C over the Avicel weight percentage in the solution .....	27
Figure 4-2 Density of DMAc/LiCl over Avicel weight percentage in the solution at 25°C and 30°C .....	28
Figure 4-3 Intrinsic viscosity of Avicel in DMAc/LiCl at 25°C and 30°C, the data point at 30°C/0.004 was excluded due to an outlier result. The diamond/triangle-shaped markers represent the intersection of the respective viscosities and therefore the intrinsic viscosities at 25°C and 30°C. The solid lines show the trendline for $\eta_{sp}/c$ results, each at 25°C and 30°C. The dashed lines belong to the $\ln(\eta_{rel})/c$ results at 25°C and 30°C. ....	30
Figure 5-1 Moisture content after exposing EmimAc to ambient air in the laboratory over time .....	34
Figure 5-2 Time for viscosity measurement of the mixtures EmimAc/H <sub>2</sub> O 85/15, EmimAc/H <sub>2</sub> O 90/10, and pure EmimAc over the Avicel weight percentage in the solution .....	35
Figure 5-3 Time for viscosity measurement of the mixtures EmimAc/DMSO at ratio 15/85 and 10/90 over the Avicel weight percentage in the solution .....	36
Figure 5-4 Time for viscosity measurement of the mixtures EmimAc/DMSO at ratio 15/85 and 10/90 compared to pure EmimAc over the Avicel weight percentage in the solution.....	37

Figure 5-5 Density measurement of EmimAc and H<sub>2</sub>O/DMSO mixtures with different ratios over Avicel weight percentage in the solution..... 38

Figure 5-6 Ratio between the relative viscosity and concentration over the Avicel concentration in the solution..... 40

Figure 5-7 Relative viscosity results over Avicel concentration in the solution ..... 41

Figure 5-8 Specific viscosity results over Avicel concentration in the solution..... 42

Figure 5-9 Calculated intrinsic viscosity of EmimAc/H<sub>2</sub>O with ratio 85/15..... 43

Figure 5-10 Calculated intrinsic viscosity of EmimAc/DMSO with ratio 10/90 at 25°C ..... 45

Figure 8-1 Specific viscosities of EmimAc/H<sub>2</sub>O, EmimAc/DMSO, and DMAc/LiCl over Avicel concentration in the solution ..... 55

Figure 8-2 Relative viscosity of EmimAc/H<sub>2</sub>O, EmimAc/DMSO, and DMAc/LiCl over Avicel concentration in the solution..... 56

Figure 8-3 Calculated intrinsic viscosity of EmimAc/H<sub>2</sub>O with ratio 90/10 ..... 56

Figure 8-4 Calculated intrinsic viscosity of EmimAc/DMSO with ratio 15/85 ..... 57

## List of Tables

Table 3-1 Cellulose product information [46].....	16
Table 3-2 EmimAc product information .....	17
Table 3-3 DMSO product information .....	17
Table 3-4 DMAc product information.....	18
Table 3-5 LiCl product information .....	18
Table 4-1 Error-values for calculated $[\eta]$ at 25°C and 30°C .....	31
Table 4-2 Used constants for molecular weight calculation, taken from literature [7] .....	32
Table 5-1 Water content of used solvents .....	33
Table 5-2 Delta max_density values for Avicel in EmimAc/water, EmimAc/DMSO, and pure EmimAc.....	39
Table 5-3 Error-values for calculated $[\eta]$ of EmimAc/H <sub>2</sub> O 85/15 and 90/10 at 25°C .....	44
Table 5-4 Error-values for calculated $[\eta]$ of EmimAc/DMSO 15/85 and 10/90 at 25°C.....	46

## List of Abbreviations

IL	Ionic liquids
MCC	Microcrystalline cellulose
DMSO	Dimethyl sulfoxide
DMF	Dimethylformamide
DMI	1,3-Dimethyl-2-imidazolidinone
EmimAc	1-Ethyl-3-methylimidazolium acetate
VOCs	Volatile organic compounds
MHS	Mark-Houwink-Sakurada
SAXS	Small angle X-ray scattering
SG	Specific gravity
RT	Room temperature
DMAc	N, N-Dimethylacetamide
LiCl	Lithium chloride



# 1 INTRODUCTION

## 1.1 State of the art / research problem

Microcrystalline cellulose (MCC) is a critical component in the field of biorefinery and sustainable technology. Derived from cellulose, the most abundant organic polymer on Earth, MCC plays a pivotal role in the transformation of biomass into valuable products. As a finely ground powder of cellulose particles, it is central to biorefinery processes that aim to fully utilize renewable resources. MCC's purpose in this context is to serve as an essential building block for various bio-based products, including biofuels, biodegradable plastics, and green chemicals, facilitating the transition toward a more sustainable and environmentally responsible industrial landscape [1, 5]. Its versatility and biocompatibility make MCC a key player in the development of eco-friendly technologies and the shift toward a bio-based economy. In the context of the global shift towards green and bio-based technologies, solubilizing MCC enables the development of innovative, sustainable products and processes in line with evolving consumer and regulatory demands. To be able to take further steps into those technologies, having the ability to produce a consistent quality of solubilized MCC is key.

In order to acquire this constant quality of dissolved MCC, it is important to understand the mechanism behind the MCC solubilizing process in different solvent systems, especially in ionic liquids (IL), as they pose the potential future of environmentally friendly solvents. McCormick *et. al* studied in 1985 the solubility of cellulose in N, N-Dimethylacetamide (DMAc)/Lithium chloride (LiCl) and calculated the molecular mass of cellulose in this mixture [7], which served then as basis for multiple works on the solubility, intrinsic viscosity, and importance of the molecular weight of cellulose. Liu, Sale *et. al* showed the superiority of 1-ethyl-3-methylimidazolium (Emim) based IL, such as Emim acetate (EmimAc), and Emim diethyl phosphate (EmimDEP), for solubilizing cellulose based on their ability to break the hydrogen bonds of the cellulose structure [30]. Minnick, Flores *et. al* introduced the ability of polar aprotic solvents including dimethyl sulfoxide (DMSO), dimethylformamide (DMF), and 1,3-dimethyl-2-imidazolidinone (DMI) as possible co-solvents for cellulose when mixed with ILs [36]. Parthasarathi, Balamurugan *et. al* reported the effects of water on the dissolution of cellulose using IL/water mixed solvent systems and their simulations show that 80:20 ratios of IL:water should be

considered as “the tipping point” above which IL-water-mixtures are equally effective on decrystallization of cellulose by disrupting the interchain hydrogen bonding interactions [39]. Le, Rudaz *et. al* published a cellulose-EmimAc-DMSO-water solvent combinations study with cellulose concentrations from 1-30wt% [27]. Koide, Wataoka *et. al* searched for heat-dissolving conditions in which the molecular weight did not decrease and the structure of cellulose in pure IL, using the small-angle X-ray scattering (SAXS) method [26]. At this time, the cellulose was rigid and linear to the extent that a rod-like approximation was established. It was also shown that the SAXS profile obtained differs depending on the dissolution conditions. Based on this result, it was assumed that the conformation of the cellulose molecule might change by changing not only the dissolution conditions but also various properties of the solvent by adding a third component, and a system in which water was added as the third component [25]. As expected, experimental results by Le, Sescousse *et. al* [28] and Parathasarathi *et al.* [39] showed that the conformation of cellulose changes depending on the content of water, which acts as a non-solvent for cellulose. These results support the conformational change of cellulose molecules due to water addition in an IL solution by molecular dynamics simulation reported by Liu *et al.* [30]. However, when mixing water and the ionic liquid EmimAc, a strong exothermic interaction is generated, which not only suggests that the solvent itself is changing its structure, but it is also possible that the properties of the mixed solvent might change [52]. Le, Rudaz *et al.* observed a stronger interaction energy between the polysaccharide chain and the IL, when using organic co-solvents, like DMSO, compared to water [27]. Koide, Urakawa *et al.* reported that, when using organic solvents, the solvent composition capable of dissolving cellulose can be set in a wider range when water is added. This is possible because of the lack of competitive formation of hydrogen bonds between the IL, cellulose, and water [25]. Those findings lead to the question, ‘how would an ionic liquid mixed solvent that uses an organic solvent instead of water behave’ and this question demands further research.

## 1.2 Purpose of the thesis / scientific question

Understanding cellulose's condition, morphology, or conformation when solubilized in ILs is important for producing a constant quality of dissolved cellulose for industrial purposes and developing/improving ways of processing cellulose. However, it is crucial to investigate the fundamentals of molecular morphology in solution further. For this purpose, simulations and viscosity measurements are needed to clarify whether the polymer exists as monomolecular

cellulose dissolved in an appropriate solvent or forms micelles in the solution, a detail that is still uncertain. The academic questions, "What kind of structure does cellulose form when dissolved in IL solvent systems? How do physical properties change and is that structure controllable?" provides the basis of this thesis. Ionic liquids and organic solvents can be employed as co-solvents in a variety of combinations, with different concentrations and conditions for dissolution. This study will be limited to the 1-Ethyl-3-methylimidazolium system, which is already known as cellulose solvent.

For each solution condition, operations such as heating and stirring are required to dissolve the cellulose in the ionic liquid. Identifying the optimal dissolution conditions, where the cellulose dissolves without reduction in molecular weight, was the first aim of this thesis. To elucidate the whole molecule and its associating structure, viscosity measurements, and solution density measurements were performed to build the foundation of further calculations. Following this, the effects of solute and water or organic solvent molecules were analyzed in detail.

### 1.3 Scope of the thesis

The objective of the thesis is to evaluate the changes in intrinsic viscosity and structural changes of MCC in aqueous and organic solvent systems through physical experiments.

The two topics that were addressed in this thesis are:

1. Determination of the molecular weight of Microcrystalline cellulose (MCC) with the Mark-Sakurada-Houwink formula based on McCormick *et al.* [7] published constants, using N, N-Dimethylacetamide (DMAc)/Lithium chloride (LiCl) mixture as a solvent system.
2. Calculation and comparison of the intrinsic viscosities of MCC solved in EmimAc, EmimAc and water, and EmimAc and Dimethyl sulfoxide (DMSO).

## 2 THEORETICAL BACKGROUND

### 2.1 Cellulose

Monocrystalline cellulose, sometimes referred to as cellulose I, is a kind of cellulose that has a highly structured and organized crystalline appearance. The other major crystalline form of cellulose, cellulose II, is less organized and more amorphous in character [38]. Cellulose I and II are the major crystalline forms of cellulose. A few hundred to thousand D-glucose units ( $C_6$  sugars) build up cellulose, a long-chained, linear polysaccharide that is joined only by -1,4-glycosidic links. The disaccharide cellobiose ( $C_{12}H_{22}O_{11}$ )<sub>n</sub> is the repeating unit in this structure (see Figure 2-1). The neighboring cellulose chains are connected by intramolecular and intermolecular hydrogen bonds, creating a crystalline, solid network. Since the cellulose chains are arranged in a structured manner, neither an enzyme nor a water molecule can pass through them. The fundamental fibrils are made of linked cellulose chains consisting of elementary fibrils. The elementary fibrils have some disordered amorphous regions in addition to the highly organized crystalline parts/areas. Elementary fibrils are highly reactive, due to their much smaller diameter and because they consist of a single, unbranched chain of cellulose molecules. Their smaller size allows for a higher surface area, providing more accessibility for chemical interactions. The reactivity of both elementary and fundamental fibrils can be influenced by factors such as cellulose source, degree of crystallinity, and the specific chemical or enzymatic treatments applied. These factors are the first pretreatment components to undergo hydrolysis. Thus, an increase in the amorphous region causes the hydrolysis rate to rise, which enhances the cellulose digestibility [49].

In order to obtain cellulose, one of two methods can be used: bottom-up cellulose biosynthesis from glucose using bacteria, such as *Acetobacter Xylinam*, or top-down cellulose production from natural sources like wood, cotton, anise plants, or other agricultural residues [49, 50]. In case of the top-down production, the extraction method, the place of origin, and the lifespan of the natural source, affect the quantity and characteristics of cellulose. These sources typically contain extractives, trace elements, cellulose, hemicellulose, and lignin. The fragile hemicellulose and lignin matrix in their cell walls are reinforced by the spirally orientated cellulose. To obtain purified cellulose, delignifying processes and other chemical treatments can be used to remove lignin, hemicellulose, and other contaminants [50].

For more than 50 years it has been known how to make MCC by acid hydrolysis from natural cellulose sources or pulp [12]. By treating cellulose, which is derived as a pulp from fibrous plant material using e.g. mineral acid, cellulose can be purified and partially depolymerized. Cellulose crystals are released during acid hydrolysis because the non-crystalline region is preferred to be hydrolyzed. The degree of polymerization (DP) of cellulose drops significantly early in the hydrolysis process, but it eventually approaches a constant DP value known as the leveling-off degree of polymerization (LODP). The LODP varies from 200 to 300 monomeric units, when using wood pulp as a source of microcrystalline cellulose. [38].

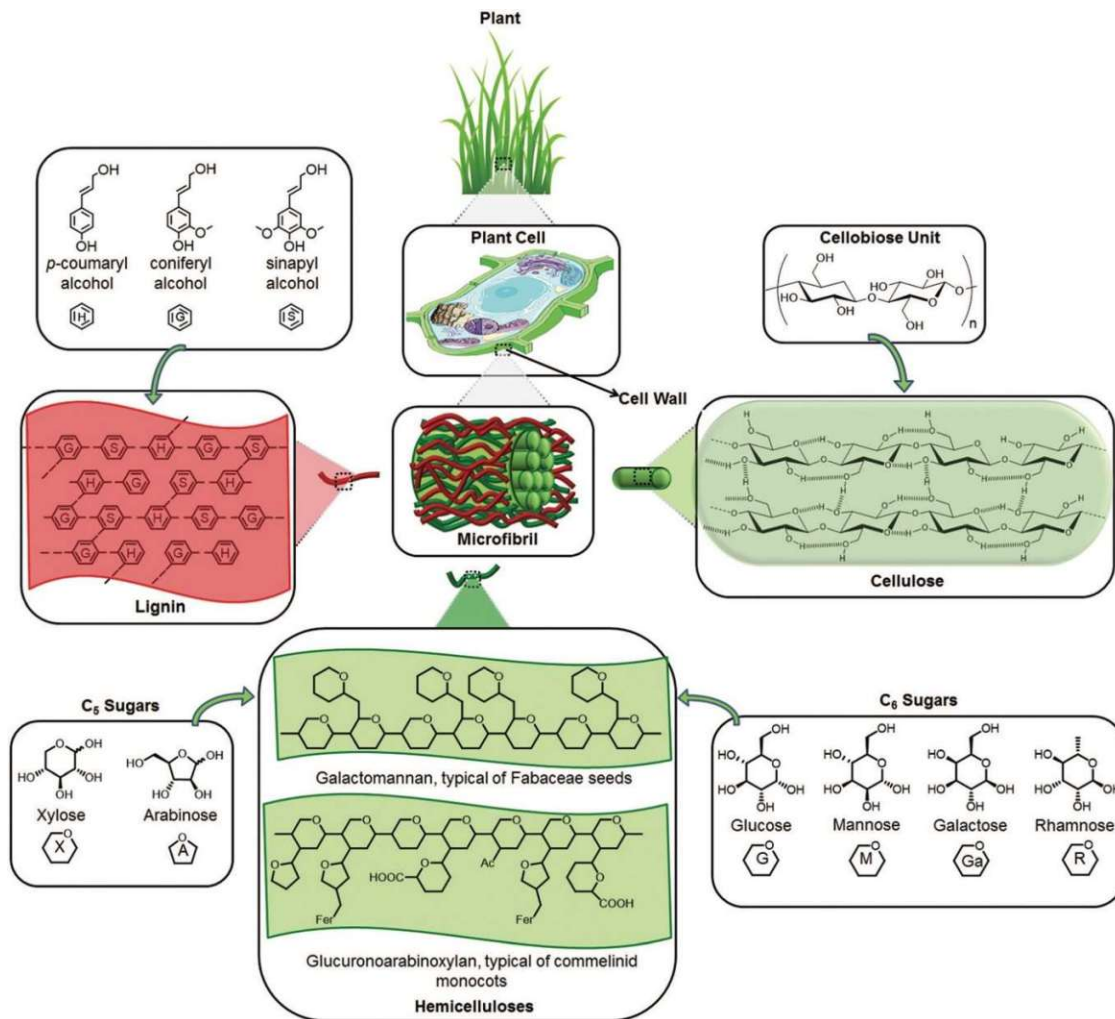


Figure 2-1 A structural section of the origin of cellulose, showing the main components of microfibril. Taken from [21]

The cellulose fibers in MCC have a diameter of a few micrometers. These fibers are made of elementary cellulose microfibrils, which have crystalline portions that are around 5 nm wide and 20–30 nm long. Crystallinity, among other characteristics, has a significant impact on the mechanical, chemical, and physical properties of cellulose [12]. For instance, as crystallinity increases, tensile strength, dimensional stability, and density rise while chemical reactivity and swelling decrease. For many years, extensive research has been conducted on the size of crystallites and the degree of cellulose crystallinity. The proportion of crystalline cellulose to the total amount of the sample material is known as the cellulose crystallinity [38, 39].

Many studies were published on the application of the produced MCC and its usage in different fields [1, 4, 10]. MCC from various sources and has been widely used as a binder and filler in medical tablets, fat replacer and stabilizer in the food industry, as well as composite material in wood and plastic industries. It also finds applications as thickening agent and emulsion stabilizer in the cosmetic industry. Cellulose is generally known for being tasteless, hydrophobic, odorless, chiral, renewable, and biodegradable [38, 50].

## 2.2 Soluble cellulose: Organic and inorganic solvents

For cellulose processing and chemical derivation, cellulose dissolution is crucial [14]. To disassemble the crystalline and amorphous parts of the cellulose, and further enable dissolving, the solvent must penetrate the cellulose structure. The solvent must break up the potent intermolecular interactions (hydrogen bonding and hydrophobic) between crystalline cellulose molecules to detangle the cellulose chains in amorphous regions (see Figure 2-2). In this case, a solvent for cellulose must possess high diffusivity, the capability to disassemble the crystalline network, and the capacity to untangle chains [19]. Numerous solvents can enter and swell cellulose and have adequate diffusivity values, but they cannot dissolve cellulose. The difficulty in overcoming the strong intermolecular interactions among cellulose molecules is thought to be the root cause of cellulose's insolubility, inhibited solvent diffusion and accessibility. Due to experimental challenges in collecting concentration profiles over time in such a small length scale, the mechanism of solvent diffusion into micron-diameter cellulose fibers is still not fully known [14, 37]. Aside from the traditional cellulose-dissolving solvents like carbon disulfide and aqueous metal salt solutions, several other compounds have been reported in recent years. These include N-methylmorpholine N-oxide monohydrate (NMMO), LiCl/N,N-dimethylacetamide (DMAc), ammonium fluorides/dimethylsulfoxide (DMSO), molten salt hydrates like

$\text{LiClO}_4 \cdot 3\text{H}_2\text{O}$  and  $\text{LiSCN} \cdot 2\text{H}_2\text{O}$ , (7-9%)NaOH/water with or without urea or thiourea added, and mixtures of ammonia or ethylenediamine and thiocyanate salts [14, 15, 41]. These solvents have been successfully employed in the production of cellulose films and fibers, with a select few also serving as homogeneous reaction media to create cellulose derivatives. However, these solvents have a number of undesirable properties that limit their commercial use, such as high toxicity, volatility, or high costs [18]. NMMO is widely used on an industrial scale as a cellulose processing solvent among the novel cellulose solvents discussed above. One of the notable advantages of using NMMO is its reversibility. The dissolution of cellulose in NMMO can be reversed, allowing for the recovery and recycling of the solvent. Also the MCC produced using NMMO is reproducible with high quality and desirable characteristics such as uniform particle size distribution [35]. These advantages align with the principles of sustainability and cost-effectiveness. On the other hand, the presence of oxidative side reactions, thermal instability, or the very high temperatures required for the dissolution process are some drawbacks of NMMO. Therefore, there is still a high demand for new "green" cellulose solvents, both for producing materials from regenerated cellulose and for the homogenous chemical derivatization. Since cellulose can dissolve in quite high concentrations (up to 15-20%) without any pre-activation, IL have been suggested as suitable cellulose solvents in this regard [14]. For the homogenous esterification of cellulose and the production of films and fibers, mainly the IL 1-butyl-3-methylimidazolium chloride (BMIMCl), EmimAc, and 1-allyl-3-methylimidazolium chloride (AmimCl) are used [53]. Ionic liquids (IL) provide a number of advantages over typical solvents because of their ionic structure, including low vapor pressure, simplicity in recycling, superior dissolving characteristics for a wide range of chemical compounds, and great thermal stability [13]. Additionally, IL can be customized to be non-volatile and non-toxic, which decreases their environmental impact [44]. They can also be made from renewable sources, which makes them more sustainable, and they require in general less energy, because temperatures below  $100^\circ\text{C}$  are sufficient during the processes [22]. Furthermore, by making minor structural modifications to the anions or cations, the characteristics of IL can be easily modified [13].

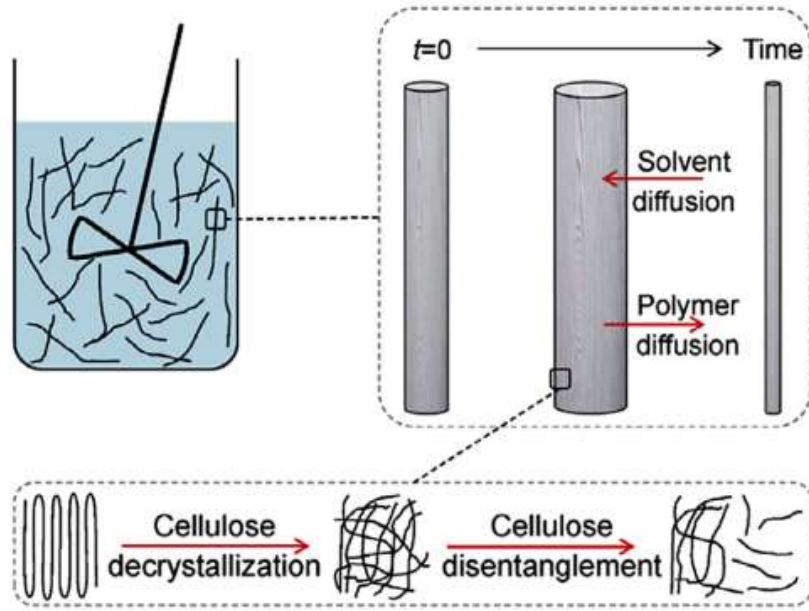


Figure 2-2 Schematic dissolution process of cellulose fibers. Taken from [14].

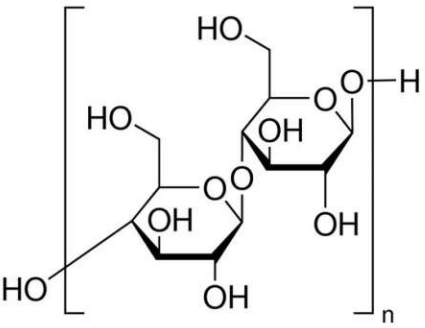
### 3 MATERIALS AND METHODS

In this chapter the origin (Table 3-1 and below), preparation (3.2) of the used materials as well as the used methods (3.3-3.4) for executed measurements, will be explained.

#### 3.1 Used materials

##### Cellulose

Table 3-1 Cellulose product information [46]

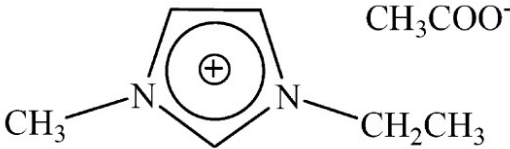
Product name/ synonyms	Avicel® PH-101, Cellulose microcrystalline, Cellulose powder, Cotton linters
Manufacturer/ Supplier	Sigma-Aldrich Japan G.K. 1-8-1 Arco Tower, Shimomeguro, Meguro-ku TOKYO 153-8927 JAPAN
Chemical structure	 <p>Figure 3-1 Chemical structure of Avicel PH-101. Taken from [46]</p>
Particle size	~50 $\mu$ m
Degree of polymerization	Ca. 200

##### Water

Distilled water was obtained from a water distillation apparatus in the laboratory.

## EmimAc

Table 3-2 EmimAc product information

Product name/ Synonyms	1-Ethyl-3-methylimidazolium acetate
Manufacturer/ Supplier	Japan Emulsifier Co., Ltd. Third Laboratory
Chemical structure	 <p>Figure 3-2 Chemical structure of EmimAc [13]</p>
Lot No.	8E28WA
Sample name	JI-63D08 *1ZQZ* and JI-63D08 *1ZQY*

## DMSO

Table 3-3 DMSO product information

Product name/ Synonyms	Dimethyl Sulfoxide
Manufacturer/ Supplier	Nacalai Tesque Inc.
Molecular formula	(CH <sub>3</sub> ) <sub>2</sub> SO
Molecular weight	78.13
Purity	≥98.0%
Grade	Nacalai 1st Grade; EP(Extra Pure Reagent)
Water content	Max. 0.2%
Density (20°C)	1.101g/ml

## DMAc

**Table 3-4 DMAc product information**

Product name/ Synonyms	N,N-Dimethylacetamide, N-Acetyldimethylamine, DMA
Manufacturer/ Supplier	Nacalai Tesque Inc.
Molecular formula	CH <sub>3</sub> CON(CH <sub>3</sub> ) <sub>2</sub>
Molecular weight	78.12
Purity	≥98.0%
Grade	Nacalai 1st Grade; EP (Extra Pure Reagent)
Density (20°C)	0.941g/ml

## LiCl

**Table 3-5 LiCl product information**

Product name/ synonyms	Lithium Chloride (Anhydrous)
Manufacturer/ Supplier	Nacalai Tesque Inc.
Molecular Formula	LiCl
Molecular weight	42.39
Purity	≥98.0%
Grade	Nacalai 1st Grade; EP(Extra Pure Reagent)
Appearance	Solid (crystal, aggregated)

## 3.2 Experimental setup / preparations

### Cellulose solubilization

Avicel was pre-dried in a drying oven at 100°C for 24hrs, based on Gericke *et al.* [13], and stored in a desiccator up to one week. A new batch was dried every week to ensure the same quality of pre-dried Avicel.

Avicel was dissolved in the EmimAc-solvent mixtures at 100°C for 1hr under constant magnetic stirring (680U/min), following preliminary studies based on literature [13, 20, 29, 36, 42]. Water absorption during the dissolving process can be neglected due to the dissolving temperature of 100°C, resulting in direct water evaporation.

Solubilization of Avicel, after the fixed time, was checked with a laser pointer to evidence light diffraction. If the solution was clear, the glass container was closed, sealed with laboratory Parafilm® (to prevent water absorption of the IL-mixture), and stirred for 24hrs at room temperature (RT) to eliminate the chance of possible precipitation caused by the temperature drop. The physical measurements started when obtaining a clear Avicel-EmimAc-solvent mixture after 24hrs.

### EmimAc

EmimAc was the main fraction of the solvent used in all experiments. There was no prior treatment before using it. It was stored at RT in an airtight plastic bottle to prevent water absorption due to its hydrophilicity.

### DMSO

DMSO was used as a co-solvent for IL-solvent mixtures and part of a one-step optimized activation for Avicel [19, 47] to dissolve it in DMAc/LiCl mixtures.

### DMAc/ LiCl

The ratio of DMAc to LiCl is based on Zhang *et al.* [52], with a molar ratio of 1:0.179. The temperature used was 100°C, and the stirring time was 1hr for the preparation of DMAc/LiCl mixtures, which was based on Rebiere *et al.* [42]. The DMAc/LiCl solvent was prepared by heating up DMAc to 40°C and slowly adding the calculated amount of LiCl with a spatula. After obtaining a clear solvent, the glass container was removed from the heat source, closed, sealed, and continuously stirred until it cooled down to RT.

The preparation of Avicel for the following solution process in DMAc/LiCl was carried out using the more time-efficient method with DMSO [19, 47], compared to the slower H<sub>2</sub>O/water/DMAc activation process. After the DMSO activation, DMSO was removed via filtration, and the remaining swollen Avicel was added to the pre-heated DMAc/LiCl mixture at 100°C. Under constant stirring with a magnetic stirrer for 1hr, the DMAc/LiCl-Avicel solution was removed from the heat, sealed with Laboratory Parafilm<sup>®</sup>, stirred until cooled down to RT, and continued stirring for 24hrs.

### Water content of used chemicals

Due to water having the most significant effect on the solubility of cellulose [25] and to help interpret and understand the measurement results, the water content of each solvent mixture was measured. A Coulometric Karl Fischer instrument was used to determine the percentage of moisture in the given sample by automated potentiometric titration with an iodine and sulfur dioxide reagent. The results are discussed in 5.1.

### 3.3 Viscosity

Absolute molecular weights are obtained using the scattering and colliding methods. The molecular weight can be determined directly from those two concepts, as mentioned in Koide *et al.* [26]. However, these methods can be costly and time-consuming. Rapid, low-cost techniques are needed to process large numbers of samples, especially regularly, which can be fulfilled by gel permeation chromatography and intrinsic viscosity. The viscosity-average molecular weight is obtained from measurements of intrinsic viscosity, which are performed in diluted solutions [48]. The viscosity-average molecular weight is a commonly used parameter in polymer science and is calculated using the Mark-Houwink-Sakurada equation. This equation relates the intrinsic viscosity  $[\eta]$  of the polymer solution to the molecular weight  $M$ , along with a set of constants for a specific polymer-solvent system [23]:

$$[\eta] = K * M^a \quad 1$$

Where  $[\eta]$  is the intrinsic viscosity of the polymer solution and  $K$  and  $a$  are constants specific to the polymer-solvent system. By measuring the intrinsic viscosity and knowing the values of

K and a for the particular polymer-solvent system, the viscosity-average molecular weight can be calculated [23].

Considering a dilute solution flowing down a capillary tube, the flow rate, and hence the shear rate, is different depending on the distance from the edge of the capillary. The polymer molecule, although small, is of finite size and “experiences” a different shear rate in different parts of its coil. This change in shear rate results in an increase in the frictional drag and rotational forces on the molecule, yielding the mechanism of viscosity increase by the polymer in the solution [48]. Based on this concept, the Ubbelohde viscometer, explained in 3.3.1, describes the viscosity in correspondence to the time based on the Hagen-Poiseuille equation as follows [44]:

$$\eta = \frac{\pi r^4 \Delta p}{8LQ} t = k * t \quad 2$$

Where r describes the radius of the capillary,  $\Delta p$  the difference of the pressure between the measured points, L is the length of the capillary, and Q is the volume flow. The constant k, which is unique for every Ubbelohde viscometer and given by the manufacturer, encapsulates these constant values.

Several other terms must be defined. The relative viscosity ( $\eta_{rel}$ ) is the ratio between the *solvent viscosity* ( $\eta_0$ ) and the viscosity of the polymer solution ( $\eta$ ) as shown in Eq. 2, and of course, the relative viscosity is a quantity larger than 1 [48].

$$\eta_{rel} = \frac{\eta}{\eta_0} \quad 3$$

The *specific viscosity*  $\eta_{sp}$  is the relative viscosity minus 1 [48]:

$$\eta_{sp} = \eta_{rel} - 1 \quad 4$$

Usually,  $\eta_{sp}$  lies between 0.2 and 0.6 for the best results. The specific viscosity, divided by the concentration and extrapolated to zero concentration, yields the *intrinsic viscosity*  $[\eta]$  [48]:

$$\left[\frac{\eta_{sp}}{c}\right]_{c=0} = [\eta] \quad 5$$

For dilute solutions, where the relative viscosity is slightly greater than unity, the following algebraic expansion is useful [48]:

$$\ln \eta_{rel} = \ln(\eta_{sp} + 1) \cong \eta_{sp} - \frac{\eta_{sp}^2}{2} + \dots \quad 6$$

Then, dividing  $\ln \eta_{rel}$  by  $c$  and extrapolating to zero concentration also yields the intrinsic viscosity [48]:

$$\left[\frac{\ln(\eta_{rel})}{c}\right]_{c=0} = [\eta] \quad 7$$

For  $[\eta]$ , two sets of units are in use. The “American” units are  $100 \text{ cm}^3/\text{g}$ , whereas the “European” units are  $\text{cm}^3/\text{g}$ . In this work, the European units are used.

### 3.3.1 Measurement

Cellulose solutions with mass percentages ranging from 0.1 to 0.5 wt% were dissolved in EmimAc solvent systems and a DMAc/LiCl solvent mixture containing 9 wt% lithium chloride (cellulose-free base). The samples' viscosity was measured in triplicate at  $25^\circ\text{C}$  for EmimAc systems and at  $30^\circ\text{C}$  for DMAc/LiCl [7] systems, with the results averaged.

Using the previously reported Mark-Houwink criteria, the average molecular weight of cellulose was calculated based on the viscosity and density measurements. Figure 3-3 shows the method used to determine  $[\eta]$  based on physical measurements. For the first question of the thesis on the molecular average weight of MCC, the provided constants  $K$  and  $a$  from McCormick *et. al.* [7] were used to calculate the molecular mass of MCC based on  $[\eta]$ .

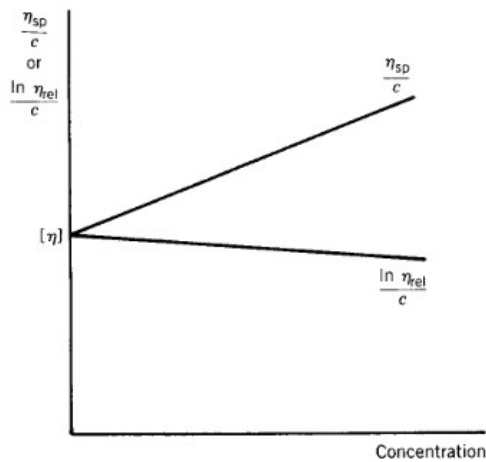


**Figure 3-3 Schematic of a plot of  $\eta_{sp}/c$  and  $\ln(\eta_{rel})/c$  versus  $c$ , and extrapolation to zero concentration to determine  $[\eta]$  [48].**

The viscosimetric approach was used to calculate the average molecular weight of cellulose using a Ubbelohde viscometer (Brand: TOP).

### Ubbelohde viscosimeter

The Ubbelohde viscometer is a device used to measure the kinematic viscosity of liquids. It consists of a narrow capillary tube connected to two reservoirs, with markings indicating a specific distance. To use it, a liquid sample is introduced into the upper reservoir, marked with line A and B, as shown in Figure 3-4. The liquid flows through the capillary tube to the lower reservoir under the influence of gravity, where the time span for the liquid to pass between the two marked points was measured. This time is then used to calculate the kinematic viscosity, either directly or through a relationship involving the dynamic viscosity and the liquid's density. Temperature control is important, as viscosity is temperature-dependent, and the water bath is used to maintain a constant temperature during testing [11]. The used water bath is a cylinder with a diameter of 35cm and a height of 45cm.

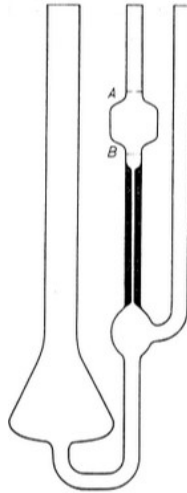


**Figure 3-4 Schematic Ubbelohde viscometer, A marks the line where the meniscus lies when the time measurement starts, and B marks the line where the time will be stopped [17]**

### 3.4 Density

The density  $\rho$  of a sample is defined as mass  $m$  divided by volume  $V$  [2]:

$$\rho = \frac{m}{V} \quad 8$$

The specific gravity  $SG$ , is calculated by dividing the density of a sample by the density of pure water at 20°C [2].

$$SG = \frac{\rho_{sample}}{\rho_{water}} \quad 9$$

Density and specific gravity values are highly temperature-dependent [2].

#### The oscillating U-tube method

The sample is introduced into a U-shaped borosilicate glass tube that is excited to vibrate at its characteristic frequency. The characteristic frequency changes depending on the density of the sample. The density of the sample can be measured through a precise determination of the characteristic frequency and a mathematical conversion [2]. The density is directly calculated by the apparatus from the quotient of the period of oscillations of the U-tube and the reference oscillator [2]:

$$density = KA * Q^2 * f_1 - KB * f_2 \quad 10$$

In the equation,  $K_A/K_B$  are the apparatus constants, given by the manufacturer, whereas  $Q$  stands for the quotient of the period of oscillation of the U-tube divided by the period of oscillation of the reference oscillator. Finally,  $f_1$  and  $f_2$  are the correction terms for temperature, viscosity, and nonlinearity.

### **Concentration measurement**

In binary mixtures, the density of the mixture is a function of its composition. Thus, by using density/concentration tables, the density value of a binary mixture can be used to calculate its composition. This is also possible with so-called quasi-binary mixtures. These mixtures contain two major components; some additional components are present in low concentrations, e.g. 1-5% or lower, compared to the two main components [2].

#### **3.4.1 Measurement**

The density measurement was done in a DMA 5000M density meter (manufacturer: Anton Paar GmbH) at 25°C for all EmimAc solvent systems. For the DMAc/LiCl solvent system, the density was additionally measured at 30°C, due to McCormick *et al.* [7], which was the basis of part one of this thesis. The result is given in  $\text{g/cm}^3$  and is used to calculate the relative viscosity.

## 4 RESULTS AND DISCUSSION – Molecular Weight of Avicel

This first part of the experiment series focused on measuring the viscosity and density of Avicel dissolved in a DMAc/LiCl system to gather the essential data to ultimately ascertain its molecular weight. Determining the molecular weight of a substance provides valuable insights about reaction mechanisms, allows predictions on how substances will behave under different conditions, and identify the physical properties. Additionally, it supports the synthesis of compounds and scaling reactions for industrial processes.

The DMAc/LiCl/Avicel mixture was measured at 25°C and at 30°C. 30°C was chosen to be able to use the constants  $K$  and  $a$ , referring to Johnston *et. al* [16], for the calculation of the molecular weight of Avicel. 25°C was chosen to be able to compare the density results of the EmimAc-based mixtures.

### 4.1 Viscosity

Figure 4-1 shows the time span measured with the Ubbelohde viscometer of DMAc/LiCl at 25°C and at 30°C over the Avicel weight percentage in the solution. The correlation between viscosity and time is given by the Hagen-Poiseuille equation (Section 3.3.1). The longer a solution needs to pass the capillary in the Ubbelohde viscosimeter, the higher its viscosity [8, 31]. The two trendlines illustrate how the viscosity of DMAc/LiCl/Avicel mixtures changes over time, in response to the increasing weight percentage of Avicel in the solution.

Based on Gericke *et al.* [13] the increasing viscosity of the DMAc/LiCl/Avicel mixtures with an increasing amount of Avicel in the solution was to be expected. The comparison between the DMAc/LiCl systems at two different temperatures shows that without Avicel in the solution, they have the same viscosity at the beginning. The first measuring point of DMAc/LiCl at 25°C and 30°C overlap completely. Without Avicel in the solution, the viscosity of DMAc/LiCl at 30°C should be lower than at 25°C though, according to Chrapava *et. al* [9]. Therefore, the first measuring result at 30°C could be an outlier. The measuring point at 0.4 wt% Avicel at 30°C shows a bigger visible gap to the trendline, with about 73s above the trendline, than at 0.1-0.3 and 0.5. The increase of viscosity per wt% Avicel in the solution is almost the same for DMAc/LiCl/Avicel at 25°C and 30°C. The viscosity increases slightly faster at 25°C to 30°C. Both systems behave almost linear with a positive increase along the x-axis.

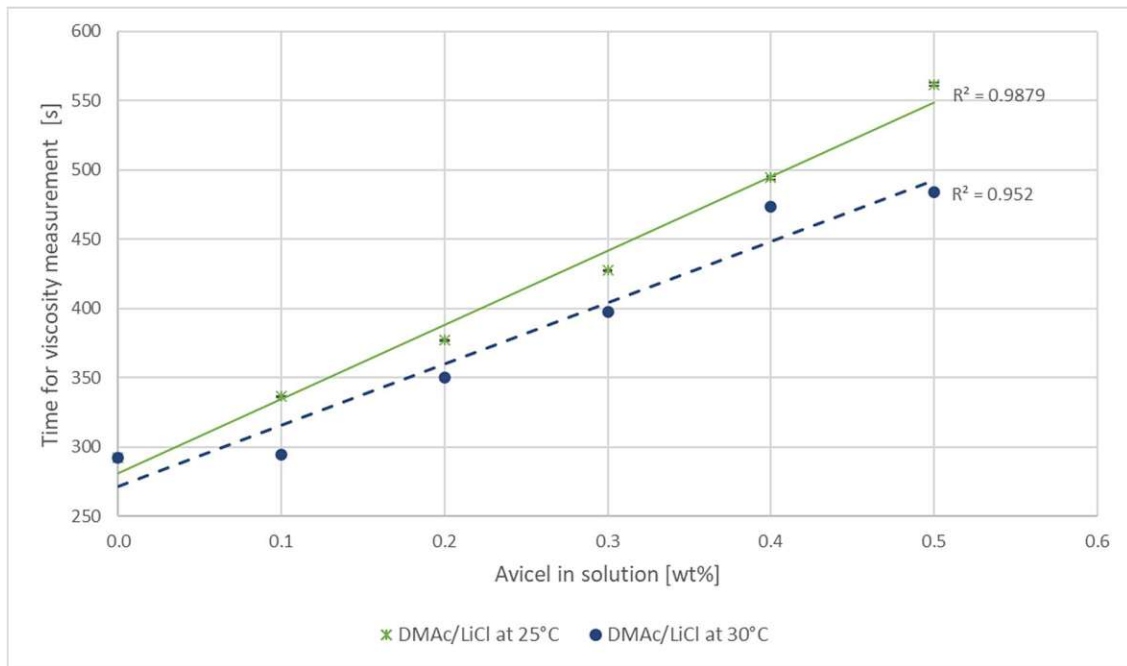


**Figure 4-1 Time for viscosity measurement of DMAC/LiCl at 25°C and at 30°C over the Avicel weight percentage in the solution**

The higher deviations at 30°C may be a result of the method used for measuring the viscosity described in 3.3.1. Due to the relatively large surface area of the water bath, a temperature difference of 5°C results in a heat transfer difference of 26W with forced convection between water and air. This estimation is based on a simplified calculation (see Appendix 8.2) and can reduce the stability of the water temperature, therefore leading to higher fluctuations in the results.

Nowadays measurements of flow times are done automatically using photosensors, e.g. Schott-Geräte (Hofheim, Germany). Since solvent viscosity is highly sensitive to temperature, a precisely controlled water bath, maintained within at least  $\pm 0.01^\circ\text{C}$  is required. An accurate temperature measurement, for example, using a well calibrated platinum resistance thermometer is crucial [17].

## 4.2 Density result evaluation

Figure 4-2 displays the measured density of the DMAC/LiCl/Avicel mixture over the weight percentage of Avicel in the solution. The solid line shows the results at 25°C, the dashed line describes the results at 30°C. It is notable that the fluctuation of the measured points at 30°C is

bigger than at 25°C. Also, the average increase in density over the 5 measurements is higher at 30°C with 0.0028, than at 25°C, with 0.0017. The standard deviation for the measured point is significantly low and not visible in the figure.

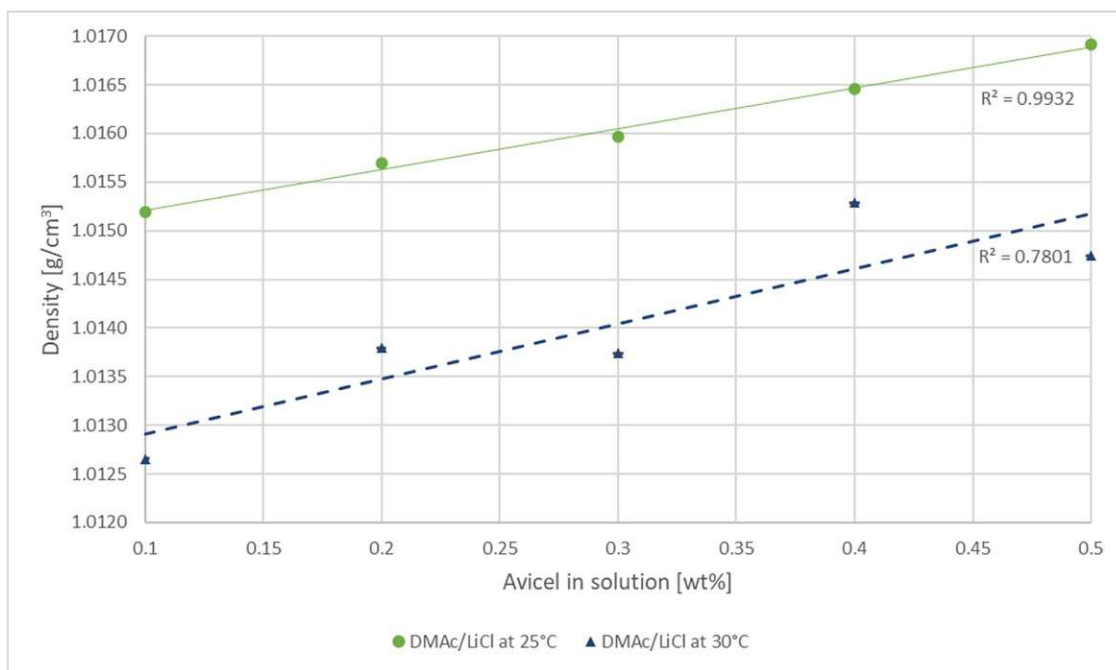


**Figure 4-2 Density of DMAC/LiCl over Avicel weight percentage in the solution at 25°C and 30°C**

Since the samples for viscosity and density measurements were prepared the same way, as described by Zhang *et al.* [52] and Rebiere *et al.* [42], random errors during preparation can be ruled out as a potential cause of measurement irregularities. However, the possibility of a systematic error affecting the whole preparation process for all samples cannot be entirely ruled out. If the error is systematic, a correction coefficient would be required to recalculate the results, however, such a coefficient has not been identified. The sample preparation process was tested multiple times in advance, evaluated during the experiments, and reassessed after the experimental stage of this study.

The calculation of the concentration is based on the solvent mass, the added Avicel mass, and the measured density. The significant change in accuracy at 30°C but not at 25°C could be caused by the density results at the higher temperature.

When the concentration of Avicel increases, the mixture becomes more viscous. A higher viscosity could affect the packing of the particles in the mixture and the way the components interact with each other at a molecular level during the density measurement. The non-Newtonian behavior of the mixture (where viscosity changes with shear rate) might cause deviations from the linear relationship between mass fraction and density [43]. The ionic interactions between LiCl and Avicel are also temperature dependent. At higher temperatures, changes in the ion pairing between LiCl and Avicel do alter the density of the solution in a non-linear way [41, 52].

### 4.3 Intrinsic viscosity result evaluation

As explained in chapter 3.3, the specific and relative viscosity was calculated, based on equations 3 and 4. The results for the specific and relative viscosity are attached in the Appendix, see Figure 8-1 and Figure 8-2.

The intrinsic viscosity is further calculated by the described method in chapter 3.3, which extrapolates the relative and intrinsic viscosity versus concentration lines until they intersect at  $x = 0$ . This intersection marks the intrinsic viscosity at a specific value on the y-axis.

Figure 4-3 shows the plotted results of the calculations for specific and relative viscosity versus the concentration of Avicel plotted over the concentration of Avicel in the solution.

As seen in Table 4-1, the obtained result for the intrinsic viscosity of Avicel at 25°C is 124.2 ml/g. The obtained result for the intrinsic viscosity of Avicel at 30°C is 92.102 ml/g.

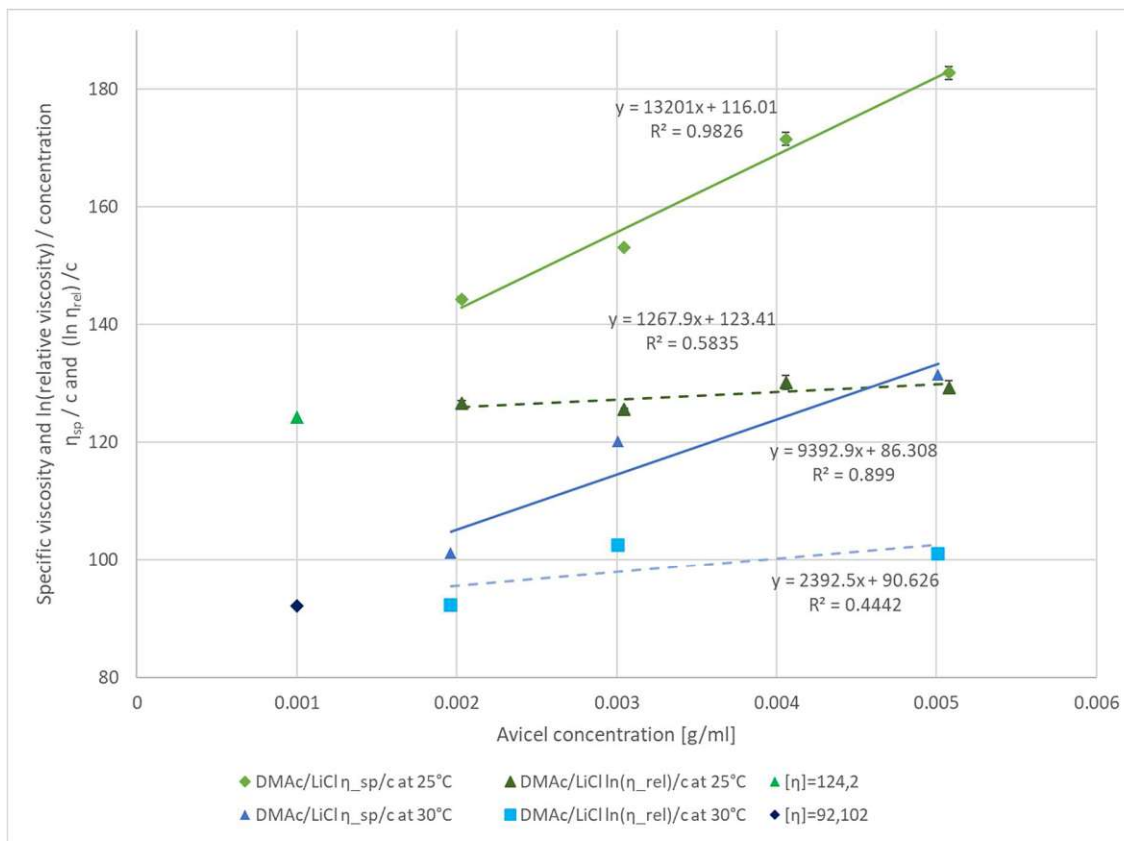


**Figure 4-3** Intrinsic viscosity of Avicel in DMAc/LiCl at 25°C and 30°C, the data point at 30°C/0.004 was excluded due to an outlier result. The diamond/triangle-shaped markers represent the intersection of the respective viscosities and therefore the intrinsic viscosities at 25°C and 30°C. The solid lines show the trendline for  $\eta_{sp}/c$  results, each at 25°C and 30°C. The dashed lines belong to the  $\ln(\eta_{rel})/c$  results at 25°C and 30°C.

Table 4-1 lists the calculated error values at 25°C and 30°C between the intersections of  $\eta_{sp}/c$  and  $\ln(\eta_{rel})/c$  with the y-axis compared to the intersection of  $\eta_{sp}/c$  and  $\ln(\eta_{rel})/c$  with each other. For both temperatures the error for  $\ln(\eta_{rel})/c$  and the y-axis is smaller compared to intersection of  $\eta_{sp}/c$  and the y-axis. This is understandable because the  $\ln(\eta_{rel})/c$  trendlines are not as steep as the  $\eta_{sp}/c$  trendlines, which results in a smaller delta for the intersection at  $y=0$ .

Compared to Hu et. al [20] and Gericke et. al [13], the trendlines for  $\eta_{sp}/c$  are plausible and behave as expected. On the other hand, the trendlines for  $\ln(\eta_{rel})/c$  do not progress as expected. The trendline should decrease with increasing Avicel concentration and not increase. The correlation between the two viscosity values is explained in chapter 3.3. Additionally,  $R^2$  of  $\ln(\eta_{rel})/c$  is for both cases, 25°C and 30°C, much lower than for  $\eta_{sp}/c$ , even though it is a solely calculated value and based on valid viscosity and density results.

**Table 4-1 Error-values for calculated  $[\eta]$  at 25°C and 30°C**

Temp. [°C]		Calculated $[\eta]$	
25		124.2	
30		92.102	
	<b>Intersection of <math>\eta_{sp}/c</math> with y-axis</b>	<b>Delta to <math>[\eta]</math></b>	<b>Error in % to the calculated intersection of the two lines with each other</b>
25	116.01	8.19	6.59
30	86.308	5.794	6.29
	<b>Intersection of <math>\ln(\eta_{rel})/c</math> with y-axis</b>		
25	123.41	0.79	0.64
30	90.626	1.476	1.6

#### 4.4 Calculation of the molecular weight of Avicel

As explained in chapter 3.3.1, equation 1 is used to calculate the intrinsic viscosity.

This equation can be further transformed to obtain the molecular weight:

$$M = a \sqrt{\frac{[\eta]}{K}} \quad 11$$

Using the constants  $a$  and  $K$  from Johnston *et. al* [16] for 9% Lithium chloride/ N, N- Dimethylacetamide at 30°C, (Table 4-1), equation 10 can be solved for the molecular mass of Avicel.

The calculated value for  $[\eta]$  at 30°C is 92.102 ml/g, with errors of 1.6-6.29%, see chapter 4.3.

**Table 4-2 Used constants for molecular weight calculation, taken from literature [7]**

T [°C]	$K \times 10^3$ [cm <sup>3</sup> /g]	$K \times 10^1$ [cm <sup>3</sup> /g]	a	Molecular weight range [kDa]
30	0.1278	54.5	1.19	125-700

Equation 11 results with the values from Table 4-2 in a molecular weight for Avicel of 252 g/mol.

## 5 RESULTS AND DISCUSSION – Calculation and comparison of the intrinsic viscosities of MCC solved in EmimAc-solvent systems

### 5.1 Water content

Due to the known hydrophilic properties of EmimAc and the significant effect of water on Avicel, all used solvents were analyzed regarding the containing water content prior to the experiments. The results are listed in **Fehler! Verweisquelle konnte nicht gefunden werden.** Additionally, the water absorption of pure EmimAc was measured over time, to eliminate the possibility of adverse effects from water absorption during the experiments, especially viscosity measurements, where the solvent system is in direct contact with humidity. The results of the water absorption over time measurement are plotted in Figure 5-1.

**Table 5-1 Water content of used solvents**

Solvent mixture [%]	Water content of solvent [wt%]
EmimAc/H <sub>2</sub> O 85/15	15.282
EmimAc/H <sub>2</sub> O 90/10	10.282
DMAc/LiCl	1.046
EmimAc/DMSO 15/85	0.553
EmimAc/DMSO 10/90	0.344
EmimAc pure IZQZ	0.332
EmimAc pure IZQY <sup>1</sup>	0.429

<sup>1</sup> Due to an EmimAc shortage of the first used batch (IZQZ), another batch (IZQY) was used to repeat some experiments to re-check measurement results.

Parathasarathi *et. al* [39] showed that a water content close to 1wt% in the solvent impacts the solubility of Avicel and changes the properties of the solution, especially for ionic liquids. For DMAc/LiCl this value is not as relevant. This is due to LiCl, being a strong desiccant, which can bind water, reducing its reactivity and preventing it from interfering with the dissolution process. This hygroscopic nature of LiCl allows the system to tolerate small amounts of water,

as it is typically bound by the LiCl, not affecting DMAc's ability to dissolve MMC. Furthermore, DMAc remains stable even in the presence of small amounts of water (around 1 wt%), as the water is mostly absorbed by LiCl and does not disrupt the solvent's properties [15, 32, 52].

As shown in Figure 5-1, water absorption is not impacting the experiment, since the critical mark of 1wt% is only reached after 100min. Therefore, during the experiments, the solvent systems/solutions were not exposed to humidity for longer than 60 min, ensuring that no negative influences from water absorption are expected.

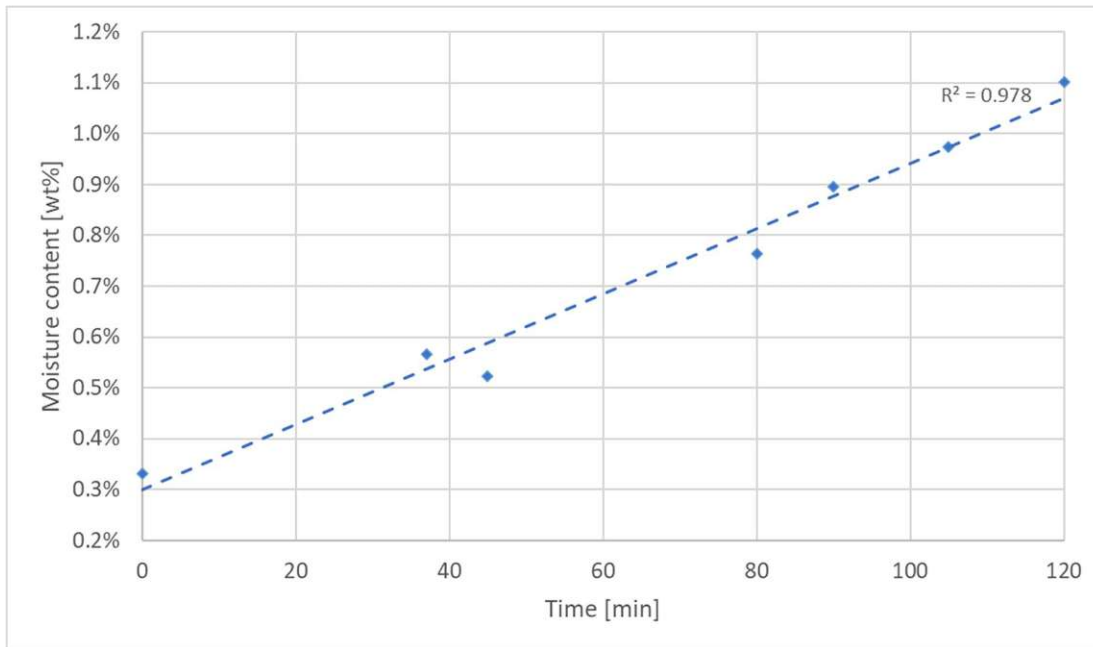


**Figure 5-1** Moisture content after exposing EmimAc to ambient air in the laboratory over time

## 5.2 Viscosity result evaluation

Figure 5-2 shows the measured time with the Ubbelohde viscometer of pure EmimAc and two different EmimAc/H<sub>2</sub>O ratios over the Avicel weight percentage in the solution. Referring to the high R<sup>2</sup> of all three mixtures, five repetitions for each data point, and the very low standard deviation, ranging from 0.07-1.6, suggest that a random error can be ruled out for this method. The impact of the humidity in the surrounding air on the viscosity of the solution systems can be ruled out as a root cause, as explained in 3.2.

The increase of the viscosity in pure EmimAc is steeper than in the two EmimAc/water mixtures. The biggest delta for the EmimAc/water 15/85 mixture is 115s and for the 10/90 mixture 145s, whereas the biggest delta for the pure EmimAc was 247s. Delta describes the difference in time between the first and last measuring point. Thus, the EmimAc/water 15/85 mixture's slopes value is 232, the 10/90 mixtures slope is 290 and pure EmimAc's slope is 494.

The pure EmimAc's viscosity increases with a slope more than double compared to the EmimAc/water 15/85 mixture. This confirms that the presence of water decreases the expansion/swelling of Avicel in EmimAc mixtures. This finding is backed by Rudaz *et al.* [44], who showed that when water is added to a cellulose–EmimAc solution above 10–15 wt%, it causes cellulose to coagulate. This occurs due to strong interactions between the IL and water. Initially, adding water increases cellulose's intrinsic viscosity in the EmimAc–water solution, due to cellulose's self-aggregation. However, further increases in water content led to coagulation. These findings highlight the critical role of solvent component interactions in understanding cellulose phase behavior [44].

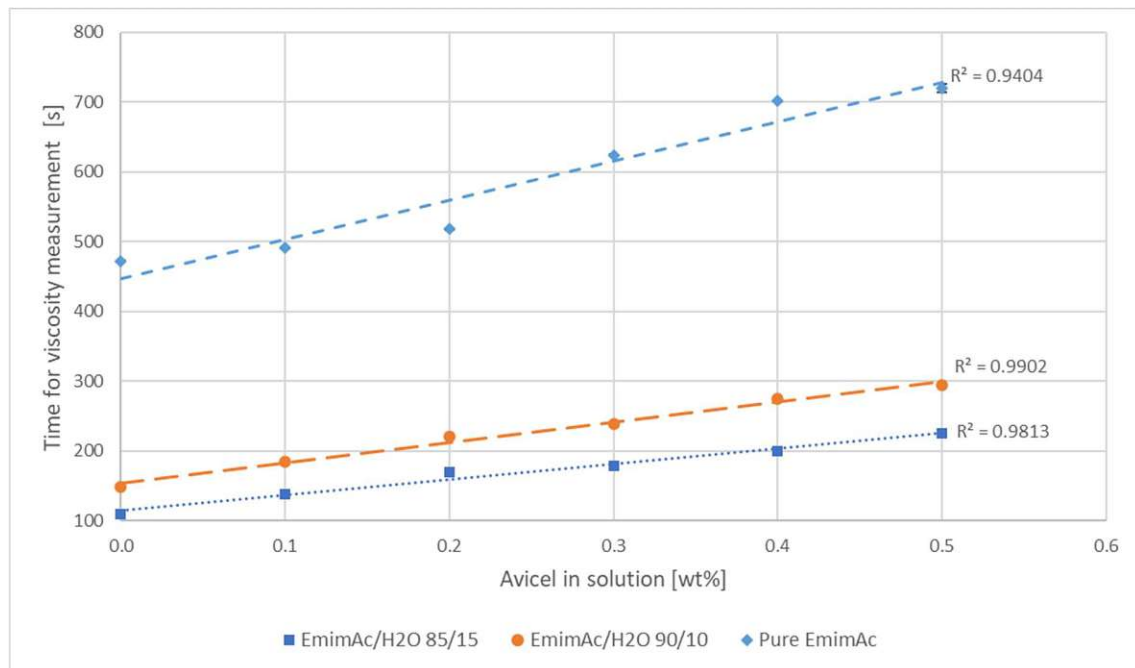


**Figure 5-2** Time for viscosity measurement of the mixtures EmimAc/H<sub>2</sub>O 85/15, EmimAc/H<sub>2</sub>O 90/10, and pure EmimAc over the Avicel weight percentage in the solution

Figure 5-3 shows the measured time with the Ubbelohde viscometer of the mixture EmimAc/DMSO in the ratios 15/85 and 10/90 over the Avicel weight percentage in the solution. The standard deviation of EmimAc/DMSO 15/85 at 0.3wt% Avicel in the solution is significantly higher compared to the other values. This could be caused by human error during sample preparation or viscosity measurement. Even though the values of 0.2wt% and 0.4wt% show a higher deviation to the trendline, the data points line up well with the other values. Including this point into the  $R^2$  calculation still yields a high value of 0.953, so the data points were kept in Figure 5-3.

The two EmimAc/H<sub>2</sub>O mixtures have an almost parallel progression. The biggest delta for the EmimAc/DMSO 15/85 mixture is 44s, and the EmimAc/DMSO 10/90 mixture shows a delta of 40s, which is way less than both of the EmimAc/water mixtures. This suggests, that DMSO solves Avicel in higher concentrations than EmimAc/water mixtures, which is supported by the work of Rudaz *et al.* [44] and Sescousse *et al* [45].

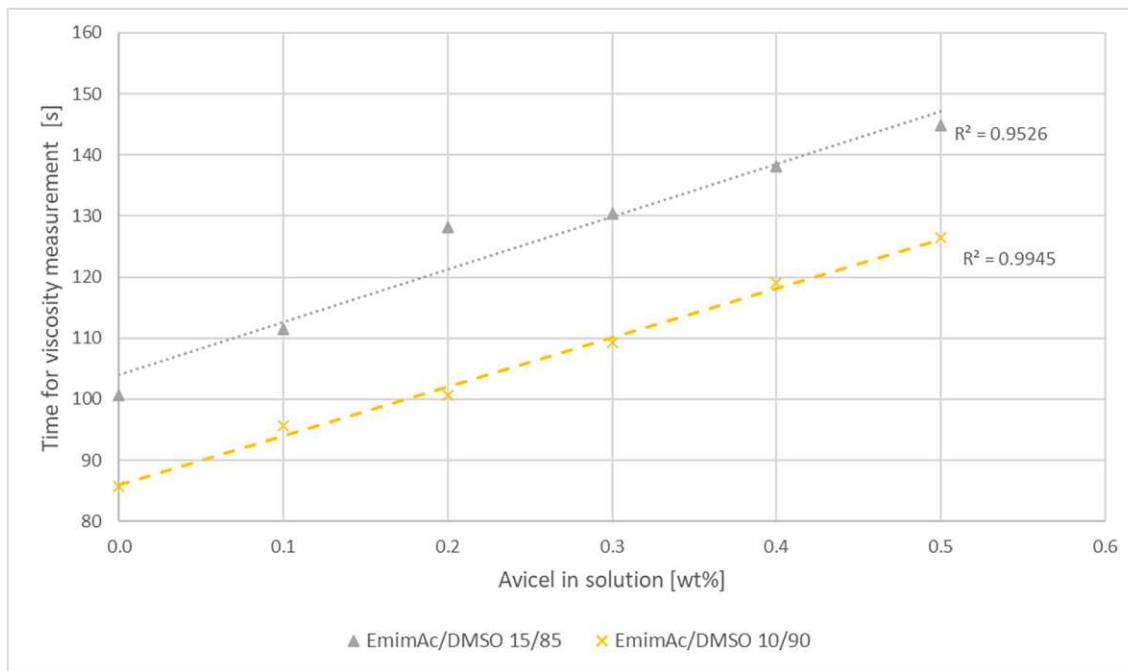


**Figure 5-3 Time for viscosity measurement of the mixtures EmimAc/DMSO at ratio 15/85 and 10/90 over the Avicel weight percentage in the solution**

Figure 5-4 shows the comparison of EmimAc/DMSO to pure EmimAc viscosity behavior. Similar to the comparison between the viscosity increase of EmimAc/water, the slope of pure EmimAc is also bigger than for the EmimAc/DMSO mixtures.

This leads to the conclusions, that DMSO does not influence the cellulose-IL interactions in the mixture [44] and that EmimAc/DMSO has the biggest capacity for solving the same amount of Avicel compared to pure EmimAc or EmimAc/water without a significant increase in viscosity. This makes the handling of EmimAc/DMSO/Avicel mixtures much easier.

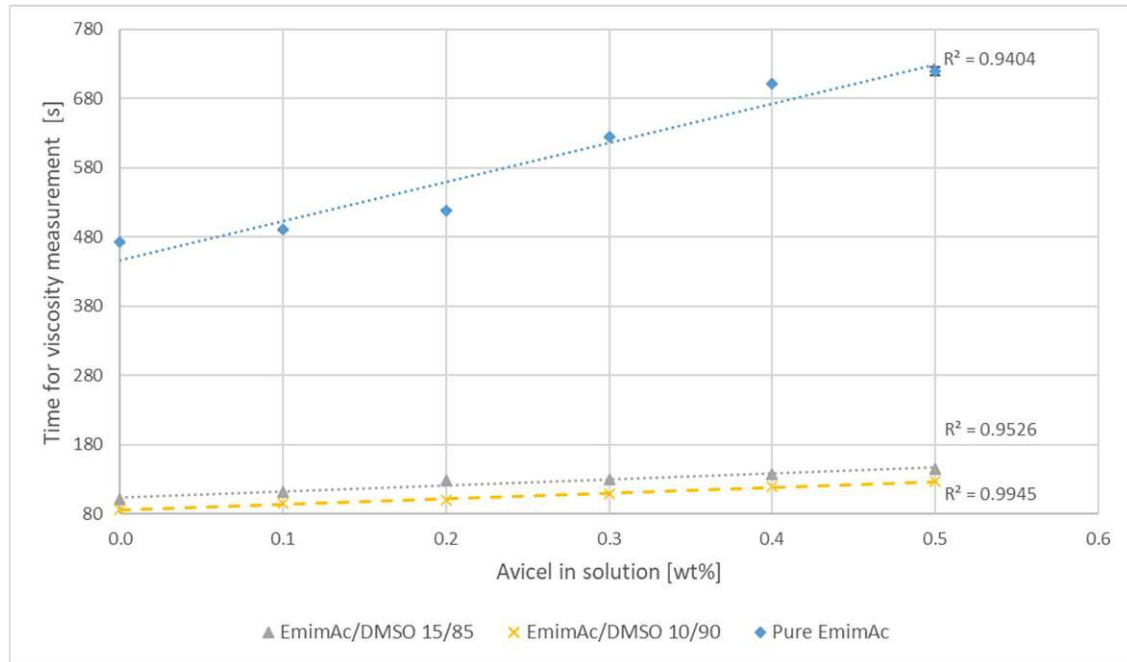


**Figure 5-4 Time for viscosity measurement of the mixtures EmimAc/DMSO at ratio 15/85 and 10/90 compared to pure EmimAc over the Avicel weight percentage in the solution**

### 5.3 Density result evaluation

The measured density values for EmimAc/water and EmimAc/DMSO mixtures over the weight percentage of Avicel in the solutions are shown in Figure 5-5. Since the measurements for density are executed by a machine and all  $R^2$  values are above 0.9, the results are considered valid.

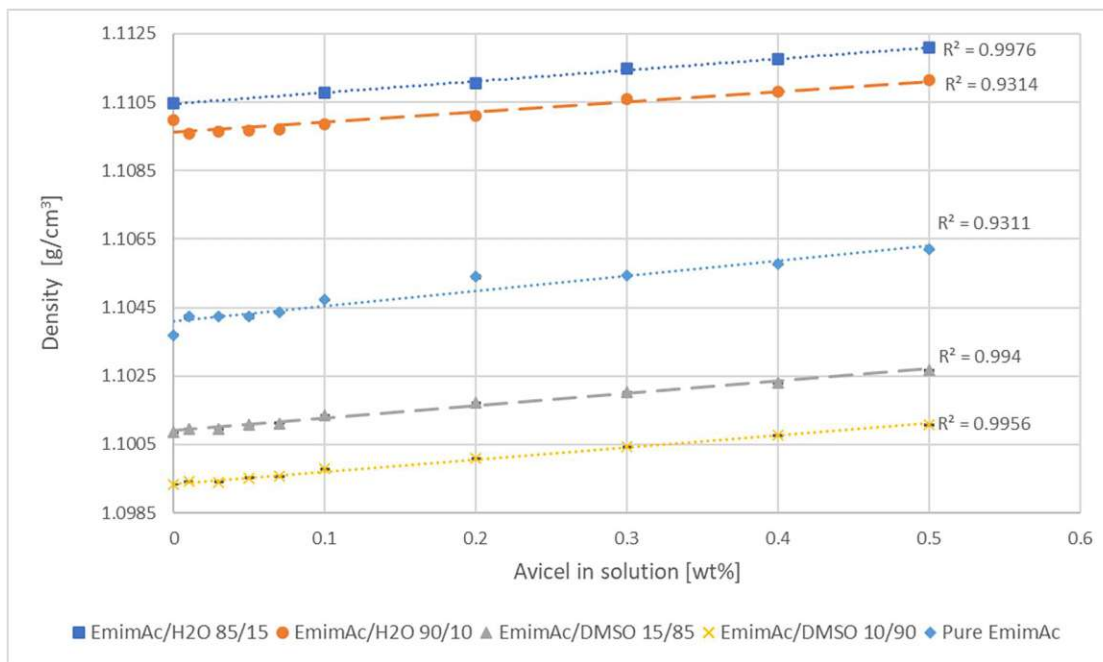


**Figure 5-5 Density measurement of EmimAc and H<sub>2</sub>O/DMSO mixtures with different ratios over Avicel weight percentage in the solution**

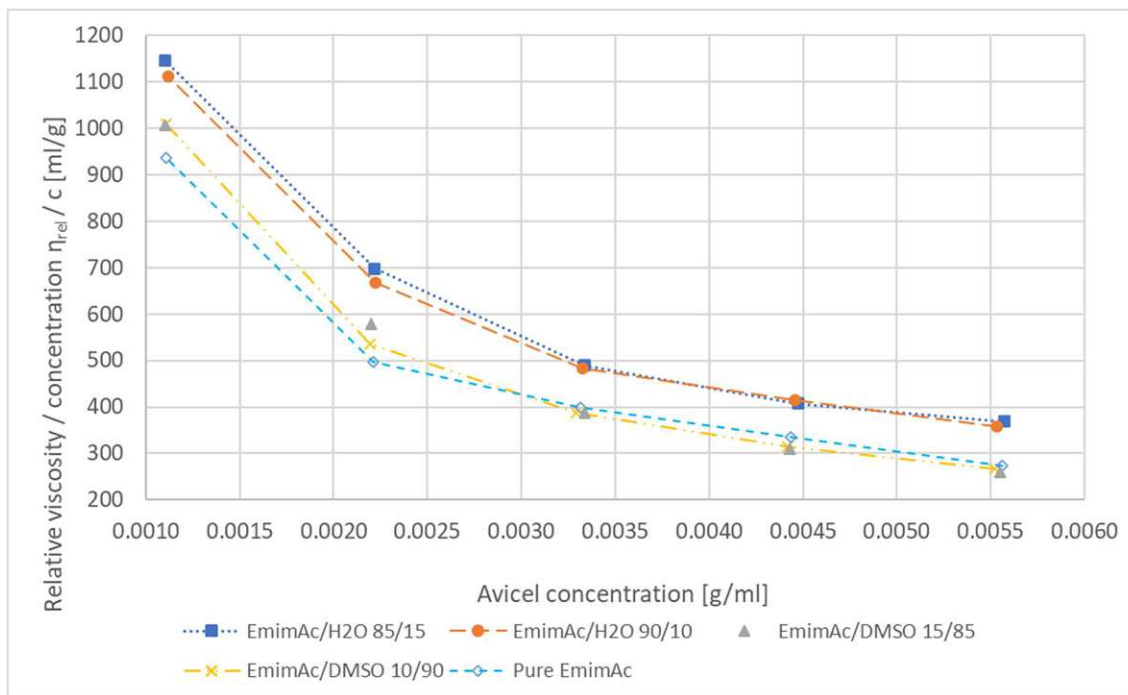
Table 5-2 lists the highest delta values for the density of the measured EmimAc/H<sub>2</sub>O/DMSO/Avicel mixtures. Delta refers to the difference between the first measuring point at 0wt% and the last measuring point at 0.5wt% Avicel. The increase in density can be expected, due to Avicel's characteristic thickening behavior during dissolution in ILs. In this comparison, the EmimAc 90/10 mixture shows the smallest increase in density with 0.00115g/cm<sup>3</sup>, compared to the pure EmimAc mixture with the biggest increase of 0.00249g/cm<sup>3</sup>. Pure EmimAc can absorb the most amount of Avicel before having Avicel coagulate compared to the other four mixtures [30, 45]. Therefore, the biggest delta in pure EmimAc can be expected. As for the difference in the two EmimAc/H<sub>2</sub>O mixtures, water increases the electron density of the solvent and promotes intramolecular hydrogen bonding in cellulose, making it stiffer [25]. Which could explain the much steeper trend for viscosity compared to density, see Figure 5-2, of the EmimAc/H<sub>2</sub>O mixtures. Hence the density appears to be less impacted by the amount of Avicel in the solution than the viscosity, it can be assumed that the most influencing factor for the intrinsic viscosity calculation is the measured viscosity in the Ubbelohde viscometer.

**Table 5-2 Delta max\_density values for Avicel in EmimAc/water, EmimAc/DMSO, and pure EmimAc**

<b>Mixture</b>	<b>Component ratio</b>	<b>Delta<sub>max</sub> [g/cm<sup>3</sup>]</b>
EmimAc/H <sub>2</sub> O	85/15	0.00157
EmimAc/H <sub>2</sub> O	90/10	0.00115
EmimAc/DMSO	18/85	0.00180
EmimAc/DMSO	10/90	0.00177
Pure EmimAc	-	0.00249

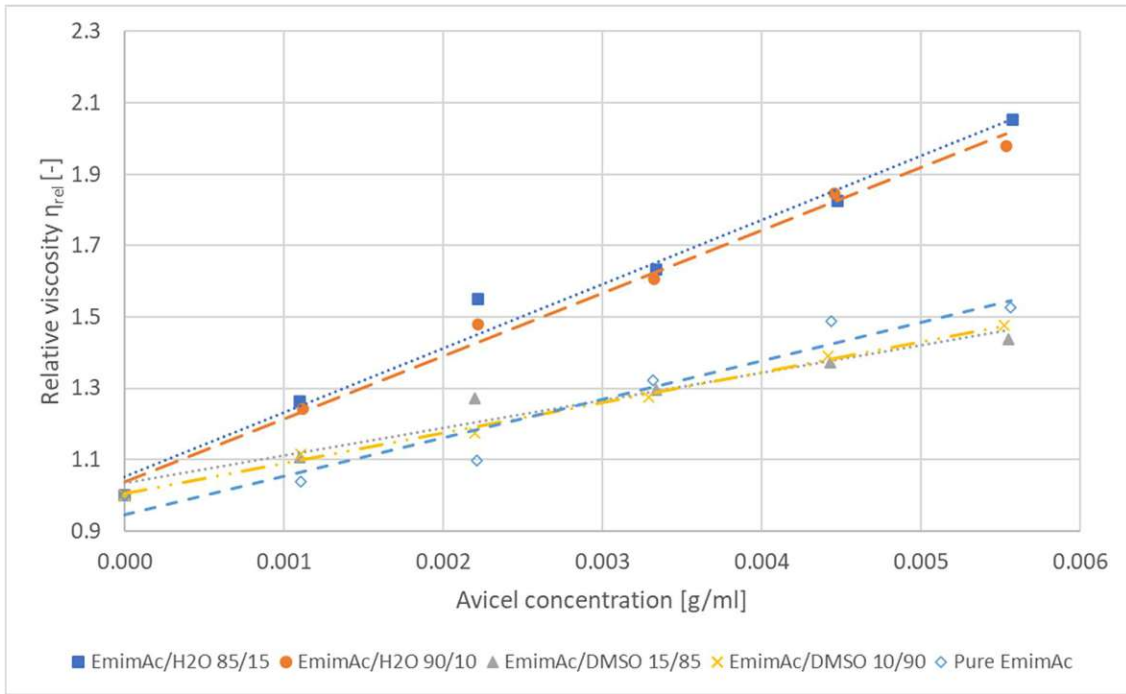
#### **5.4 Intrinsic viscosity results evaluation**

The trend of all EmimAc mixtures with Avicel follows the same decreasing path. Figure 5-6 shows that the ratio between relative viscosity per concentration of Avicel decreases over the concentration of Avicel in the solution. The results were expected, as this graph serves as a control to the calculation. The results are decreasing, since the relative viscosity is inversely proportional to concentration and plotted over an increasing Avicel concentration. Therefore, if the trend of the results looked different, it would indicate an error.



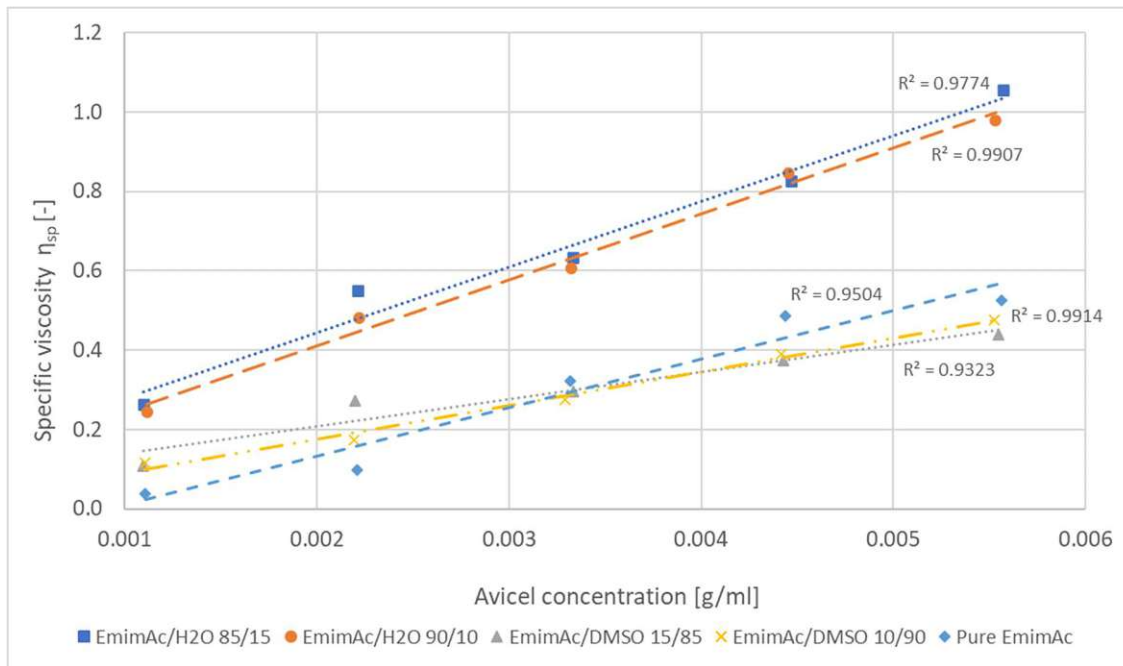
**Figure 5-6 Ratio between the relative viscosity and concentration over the Avicel concentration in the solution**

Figure 5-7 shows the calculated relative viscosity of EmimAc/H<sub>2</sub>O/DMSO mixtures with different ratios over Avicel concentration in the solution. Compared to Gericke *et al.* [13] the progression of data points for the relative viscosity is rather linear until the mixture reaches a concentration of 1g/ml of Avicel. Just after that, the progression starts to show an exponential character. Since the measurement points in this experiment lie between a concentration of 0-0.006 g/ml of Avicel in the solution, the linear increasing character of the results comply with literature [13, 45].



**Figure 5-7 Relative viscosity results over Avicel concentration in the solution**

Figure 5-8 shows the calculated specific viscosity of EmimAc/H<sub>2</sub>O/DMSO mixtures with different ratios over Avicel concentration in the solutions. Compared to Hu *et. al* [20], the progression of the specific viscosity is expected to be linear. In this case, the approach of the results towards  $R^2 = 1$  indicates valid results.



**Figure 5-8 Specific viscosity results over Avicel concentration in the solution**

Figure 5-9 shows the results representative for both EmimAc/H<sub>2</sub>O mixtures and the EmimAc/DMSO 15/85 mixture and Figure 5-10 display the results for EmimAc/DMSO 10/90. In all of them, except for EmimAc/DMSO 10/90 shown in Figure 5-10, the  $\eta_{sp}/c$  line should have an ascending character [20, 48, 50, 54]. The measured values represent the solutions' Avicel concentration, viscosity, and density. All other values were taken from further calculations, based on the measurements. In previous figures, it was shown that the measurement method is robust and delivers seemingly valid results. Additionally, the preparation of all samples was conducted using the same process and was excessively tested beforehand. Further details are shown in chapter 3.2 Experimental setup / preparations.

The errors of the calculations are listed in Table 5-3 and Table 5-4. The errors lie between 0.04%, for EmimAc/DMSO 10/90, and 18.5% for EmimAc/H<sub>2</sub>O 90/10. The errors represent the delta between the calculated intersection of  $\eta_{sp}/c$  and  $\ln(\eta_{rel})/c$  with each other, which corresponds to the intrinsic viscosity  $[\eta]$ , and the intersection points of the y-axis with  $\eta_{sp}/c$  and  $\ln(\eta_{rel})/c$  separately. The solutions containing EmimAc and water were underlying greater fluctuations throughout the whole experimental series. This can be caused by the effects of water on the solubility of cellulose, as explained in 2.1.

For all mixtures, except EmimAc/DMSO 10/90, the intersection point between  $\eta_{sp}/c$  and  $\ln(\eta_{rel})/c$  lines, is located on the left to the y-axis. This could be caused by measurement inaccuracies. Ideally, the graphs should look alike to Figure 3-3, respectively Figure 5-10.

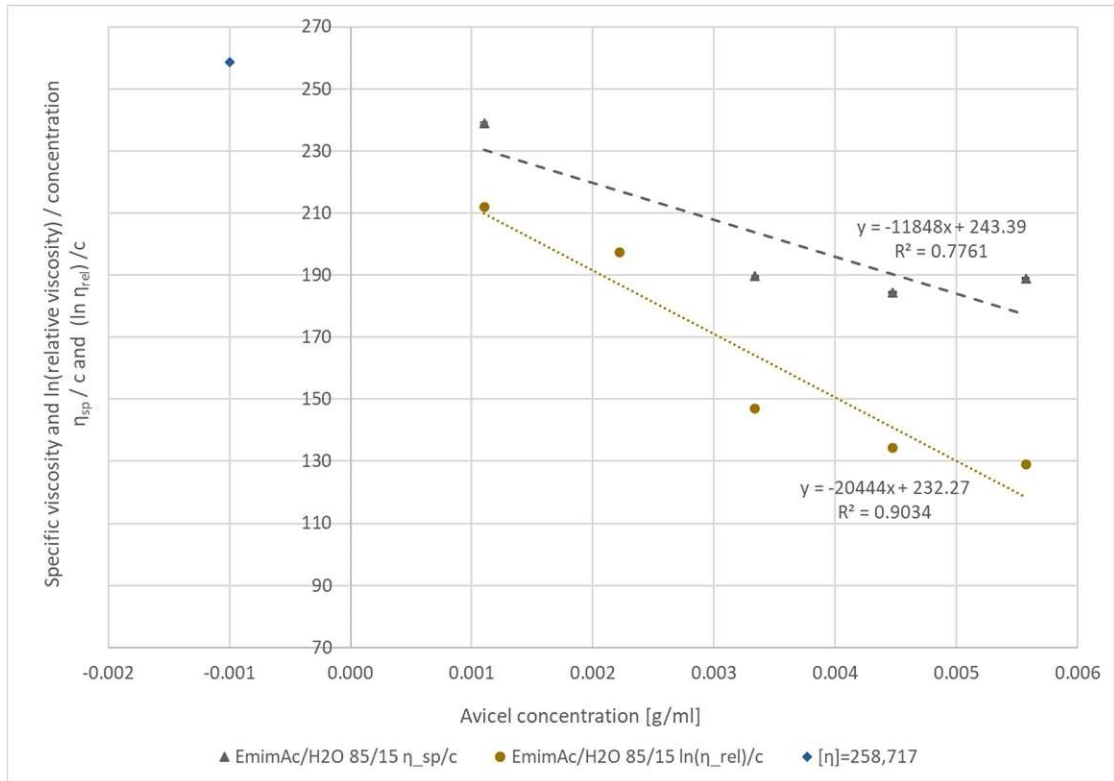


**Figure 5-9** Calculated intrinsic viscosity of EmimAc/H<sub>2</sub>O with ratio 85/15

The graphs for the EmimAc/H<sub>2</sub>O 90/10 and EmimAc/DMSO 15/85 mixture are in the Appendix, see Figure 8-3 and Figure 8-4. Table 5-3 lists the calculated values for both EmimAc/H<sub>2</sub>O mixtures for comparison. The inclination of  $\eta_{sp}/c$  is expected to increase with the Avicel concentration in the solution. However, the results tend to follow the linear trendline. Additionally, the previous measurements and calculation seem to be valid. The standard deviations are so small that they are almost not visible in the graph, even though they are included. This suggests that the small measurement errors, which are not noticeable during the first stages of calculation accumulate and lead to significant changes in the final calculation step for  $[\eta]$ .

**Table 5-3 Error-values for calculated  $[\eta]$  of EmimAc/H<sub>2</sub>O 85/15 and 90/10 at 25°C**

85/15 mixture			90/10 mixture		
calculated $[\eta]$	delta to $[\eta]$	error in %	calculated $[\eta]$	delta to $[\eta]$	error in %
258.72			257.641		
Intersection of $\eta_{sp}/c$ with y-axis					
243.39	15.327	5.92	229.23	28.411	11.03
Intersection of $\ln(\eta_{rel})/c$ with y-axis					
232.27	26.447	10.22	209.97	47.671	18.50

Even though water and humidity can be a problem for the hydrophilic EmimAc and therefore could be a problem for solving Avicel [25], this factor was shown to be not relevant for this set of measurements, explained in 5.1 Water content. Water decreases the expansion/swelling of Avicel in EmimAc mixtures and leads to coagulation [28]. This fact is especially relevant for the EmimAc/H<sub>2</sub>O solutions. It was less of a problem for EmimAc/DMSO solutions, evident from Figure 8-3 and Figure 5-10. That is due to DMSO's capability of solving Avicel in higher concentrations, backed by Sescousse *et al* [45]. The temperature issue is evident in the DMAc/LiCl/Avicel solutions as well, as with an increasing temperature the stability of the system and the measured results decrease. More fluctuations and rogue results occur at 30°C compared to 25°C, for viscosity as well as density measurements. The observed higher deviations at 30°C can be attributed to the measurement method used for viscosity, potentially causing instability in the water temperature and leading to fluctuations in the results and therefore draw the connection to the further calculated values. As the concentration of Avicel increases, the viscosity of the mixture also rises, which can affect the packing of the particles and the interactions at the molecular level during density measurements [27]. Additionally, the non-Newtonian behavior of the mixture, where viscosity changes with shear rate, can introduce deviations from a linear relationship between mass fraction and density. Furthermore, the ionic interactions between LiCl and Avicel, which are temperature-dependent, contribute to non-linear changes in the density of the solution, especially at higher temperatures. These factors combined suggest that both physical properties of the mixture introduce complexities that need to be carefully

considered. Therefore,  $\eta_{rel}$  and subsequently  $\eta_{sp}$  are a combination of viscosity and density results, previously explained causes can be at fault for the unexpected behavior.

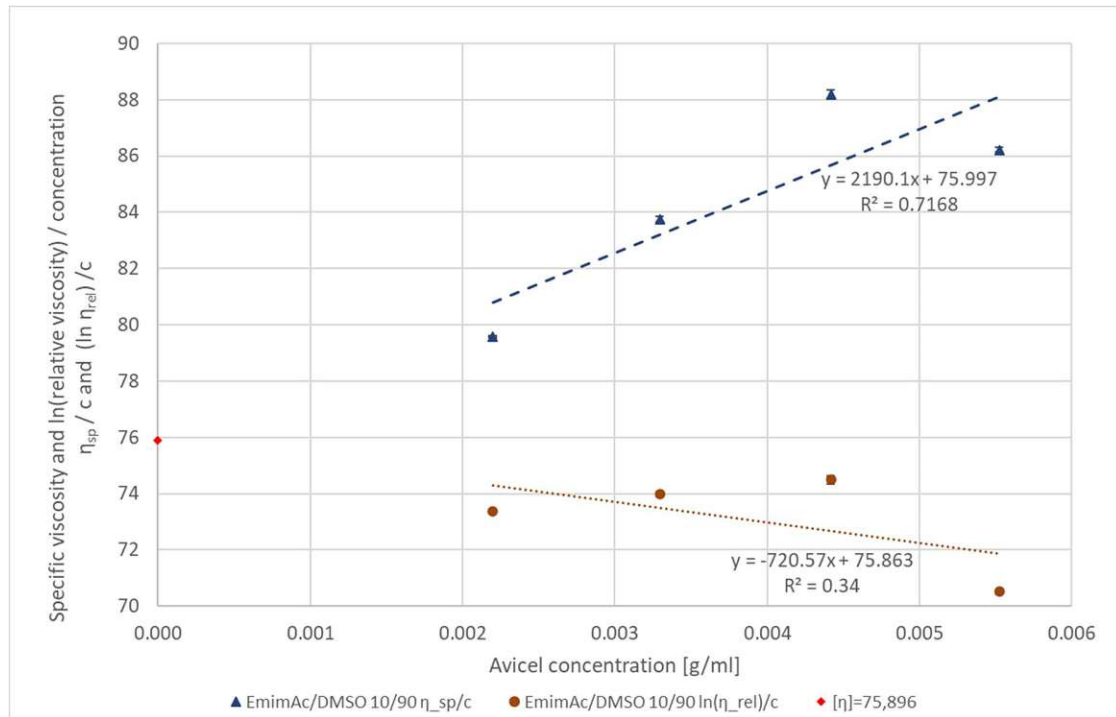


**Figure 5-10** Calculated intrinsic viscosity of EmimAc/DMSO with ratio 10/90 at 25°C

The errors for both EmimAc/DMSO mixtures show lower errors compared to the EmimAc/water mixtures. Especially the 10/90 mixture, as shown in Figure 5-10, picture the expected results according to literature [20, 24]. However, the low errors on intersections with the y-axis, as shown in Table 5-4, and the seemingly valid graph do not comply with the low  $R^2$  of  $\ln(\eta_{rel})/c$ .

**Table 5-4 Error-values for calculated  $[\eta]$  of EmimAc/DMSO 15/85 and 10/90 at 25°C**

15/85 mixture			10/90 mixture		
calculated $[\eta]$	delta to $[\eta]$	error in %	calculated $[\eta]$	delta to $[\eta]$	error in %
110.089			75.896		
Intersection of $\eta_{sp}/c$ with y-axis					
102.08	8.009	7.28	75.997	0.101	0.13
Intersection of $\ln(\eta_{rel})/c$ with y-axis					
99.51	10.579	9.61	75.863	0.033	0.04

## 6 CONCLUSION

This work aims to understand the molecular structure and morphology of cellulose dissolved in ionic liquids, especially focusing on 1-Ethyl-3-methylimidazolium (EmimAc) systems. Viscosity analysis and solution density measurements were used to investigate the intrinsic viscosity and structural changes of microcrystalline cellulose (MCC) in aqueous and organic solvent systems. The study focuses on two key topics: determining MCC's molecular weight by using the Mark-Sakurada-Houwink formula and analyzing the effects of temperature, water content, and solvent composition on viscosity in EmimAc/H<sub>2</sub>O/DMSO mixtures. For the first key topic, the calculated intrinsic viscosity for MCC is 252 g/mol.

For the second key topic, the finding revealed that, even small temperature changes, such as 0.01°C, cause significant fluctuations, especially at higher temperatures. The measurements with DMAc/LiCl/Avicel at 25°C had errors for the calculated  $\eta_{sp}/c$  and  $\ln(\eta_{rel})/c$  of 6.59% and 0.64%, with coefficients of determination of 0.98 and 0.58. At 30°C, these errors were 6.29% and 1.6%, with coefficients of determination of 0.9 and 0.44, highlighting decreased stability at higher temperatures.

The water content played a crucial role, as shown by a 5wt% difference in H<sub>2</sub>O between the EmimAc/H<sub>2</sub>O 15/85 and 10/90 mixtures with the same amount of 2wt% Avicel leading to a difference of 30 seconds in viscosity measurements using an Ubbelohde viscometer. Water reduced Avicel swelling in EmimAc mixtures, causing coagulation, while DMSO mitigated this effect. Among the tested solvent systems EmimAc/DMSO 10/90 had the highest capacity for dissolving Avicel because DMSO does not influence the cellulose-IL interactions in the mixture.

Overall, higher Avicel concentrations increased viscosity, affecting molecular interactions and density, especially if water is a part of the mixture. Additionally, temperature-sensitive ionic interactions contributed to non-linear density changes. These combined factors complicated measurements and result interpretation.

The experimental work was significantly influenced and constrained by time limitations, fluctuations in laboratory humidity, caused by humid summer conditions and the characteristics of

Japanese construction design, as well as the available methods to use for viscosity measurements. These factors may have affected the consistency and reproducibility of the dissolution and analysis processes, potentially affecting some results.

This study highlights the importance of understanding the cellulose solvating behavior in ionic liquids and its solvent systems. Also, it shows that water plays a crucial role in altering the conformation of cellulose and its interaction with the solvent. Therefore, future research should focus on gaining more knowledge of hydrogen-bonding properties of those systems, temperature dependent solvating mechanisms of Avicel as well as viscosity modifying structural behaviors. More controlled solubilizing conditions could lead to higher efficiencies in processing Avicel.

## 7 References

- [1] Mehran Alavi. 2019. Modifications of microcrystalline cellulose (MCC), nanofibrillated cellulose (NFC), and nanocrystalline cellulose (NCC) for antimicrobial and wound healing applications. *e-Polymers* 19, 1, 103–119. DOI: <https://doi.org/10.1515/epoly-2019-0013>.
- [2] Anton Paar GmbH. 2012. *Instruction Manual DMA 5000M*. pdf, C76IB003EN-E. Retrieved from.
- [3] Hans D. Baehr and Stephan Kabelac. 2012. *Thermodynamik*. Springer Berlin Heidelberg, Berlin, Heidelberg.
- [4] Sneh P. Bangar, Okon J. Esua, C. Nickhil, and William S. Whiteside. 2023. Microcrystalline cellulose for active food packaging applications: A review. *Food Packaging and Shelf Life* 36, 101048. DOI: <https://doi.org/10.1016/j.fpsl.2023.101048>.
- [5] Jaya Baranwal, Brajesh Barse, Antonella Fais, Giovanna L. Delogu, and Amit Kumar. 2022. Biopolymer: A Sustainable Material for Food and Medical Applications. *Polymers* 14, 5. DOI: <https://doi.org/10.3390/polym14050983>.
- [6] Shubhankar Bhattacharyya and Faiz U. Shah. 2018. Thermal stability of choline based amino acid ionic liquids. *Journal of Molecular Liquids* 266, 597–602. DOI: <https://doi.org/10.1016/j.molliq.2018.06.096>.
- [7] Charles L. McCormick, Peter A. Callais, Brewer H. Hutchinson, Jr. 1985. *Solution Studies of Cellulose in Lithium Chloride and N,N-Dimethylacetamide*. paper, S03, 7446-11-9; Rytan V-1, 25212-74-2. Retrieved from.
- [8] Siyoung Q. Choi, Kyuhan Kim, Colin M. Fellows, Kathleen D. Cao, Binhua Lin, Ka Y. C. Lee, Todd M. Squires, and Joseph A. Zasadzinski. 2014. Influence of molecular coherence on surface viscosity. *Langmuir : the ACS journal of surfaces and colloids* 30, 29, 8829–8838. DOI: <https://doi.org/10.1021/la501615g>.
- [9] Sarka Chrapava, Didier Touraud, Thomas Rosenau, Antje Potthast, and Werner Kunz. 2003. The investigation of the influence of water and temperature on the LiCl/DMAc/cellulose system. *Phys. Chem. Chem. Phys.* 5, 9, 1842–1847. DOI: <https://doi.org/10.1039/B212665F>.
- [10] D. Lavanya, P.K. Kulkarni, M. Dixit, P.K. Raavi, and L.N.V. Krishna. 2011. *Sources of cellulose and their applications- A review*, 2.

- [11] J. Einfeldt. 1970. Zur Kapillarviskosimetrie verdünnter Lösungen. *Rheol Acta* 9, 3, 429–434. DOI: <https://doi.org/10.1007/BF01975412>.
- [12] Keiran Fleming, Derek G. Gray, and Stephen Matthews. 2001. Cellulose Crystallites. *Chem. Eur. J.* 7, 9, 1831–1836. DOI: [https://doi.org/10.1002/1521-3765\(20010504\)7:9<1831:AID-CHEM1831>3.0.CO;2-S](https://doi.org/10.1002/1521-3765(20010504)7:9<1831:AID-CHEM1831>3.0.CO;2-S).
- [13] Martin Gericke, Kerstin Schlufner, Tim Liebert, Thomas Heinze, and Tatiana Budtova. 2009. Rheological properties of cellulose/ionic liquid solutions: from dilute to concentrated states. *Biomacromolecules* 10, 5, 1188–1194. DOI: <https://doi.org/10.1021/bm801430x>.
- [14] Mohammad Ghasemi, Marina Tsianou, and Paschalis Alexandridis. 2017. Assessment of solvents for cellulose dissolution. *Bioresource technology* 228, 330–338. DOI: <https://doi.org/10.1016/j.biortech.2016.12.049>.
- [15] Adam S. Gross, Alexis T. Bell, and Jhih-Wei Chu. 2013. Preferential interactions between lithium chloride and glucan chains in N,N-dimethylacetamide drive cellulose dissolution. *The journal of physical chemistry. B* 117, 12, 3280–3286. DOI: <https://doi.org/10.1021/jp311770u>.
- [16] H. Kirk Johnston, S. Sourirajan. 1972. Mark-Houwink Constants for Some Cellulose Acetate-Organic Solvent Systems 16, 3375–3380.
- [17] S. E. Harding. 1997. The intrinsic viscosity of biological macromolecules. Progress in measurement, interpretation and application to structure in dilute solution. *Progress in biophysics and molecular biology* 68, 2-3, 207–262. DOI: [https://doi.org/10.1016/S0079-6107\(97\)00027-8](https://doi.org/10.1016/S0079-6107(97)00027-8).
- [18] Ute Henniges, Mirjana Kostic, Andrea Borgards, Thomas Rosenau, and Antje Potthast. 2011. Dissolution behavior of different celluloses. *Biomacromolecules* 12, 4, 871–879. DOI: <https://doi.org/10.1021/bm101555q>.
- [19] Ute Henniges, Philipp Vejdovszky, Martin Siller, Myung-Joon Jeong, Thomas Rosenau, and Antje Potthast. 2014. Finally Dissolved! Activation Procedures to Dissolve Cellulose in DMAc/LiCl Prior to Size Exclusion Chromatography Analysis – A Review. *CCHG* 1, 1, 52–68. DOI: <https://doi.org/10.2174/2213240601666131118220030>.
- [20] Hao Hu, Akihiko Takada, and Yoshiaki Takahashi. 2014. Intrinsic Viscosity of Pullulan in Ionic Liquid Solutions Studied by Rheometry. *J. Soc. Rheol., Jpn* 42, 3, 191–196. DOI: <https://doi.org/10.1678/rheology.42.191>.

- [21] Furkan H. Isikgor and C. R. Becer. 2015. Lignocellulosic biomass: a sustainable platform for the production of bio-based chemicals and polymers. *Polym. Chem.* 6, 25, 4497–4559. DOI: <https://doi.org/10.1039/C5PY00263J>.
- [22] Mohammad R. Kasaai. 2002. Comparison of various solvents for determination of intrinsic viscosity and viscometric constants for cellulose. *J. Appl. Polym. Sci.* 86, 9, 2189–2193. DOI: <https://doi.org/10.1002/app.11164>.
- [23] Mohammad R. Kasaai. 2007. Calculation of Mark–Houwink–Sakurada (MHS) equation viscometric constants for chitosan in any solvent–temperature system using experimental reported viscometric constants data. *Carbohydrate polymers* 68, 3, 477–488. DOI: <https://doi.org/10.1016/j.carbpol.2006.11.006>.
- [24] Mürşide Kes and Bjørn E. Christensen. 2013. A re-investigation of the Mark-Houwink-Sakurada parameters for cellulose in Cuen: a study based on size-exclusion chromatography combined with multi-angle light scattering and viscometry. *Journal of chromatography. A* 1281, 32–37. DOI: <https://doi.org/10.1016/j.chroma.2013.01.038>.
- [25] Mitsuharu Koide, Hiroshi Urakawa, Kanji Kajiwara, Thomas Rosenau, and Isao Wataoka. 2020. Influence of water on the intrinsic characteristics of cellulose dissolved in an ionic liquid. *Cellulose* 27, 13, 7389–7398. DOI: <https://doi.org/10.1007/s10570-020-03323-2>.
- [26] Mitsuharu Koide, Isao Wataoka, Hiroshi Urakawa, Kanji Kajiwara, Ute Henniges, and Thomas Rosenau. 2019. Intrinsic characteristics of cellulose dissolved in an ionic liquid: the shape of a single cellulose molecule in solution. *Cellulose* 26, 4, 2233–2242. DOI: <https://doi.org/10.1007/s10570-018-02238-3>.
- [27] Kim A. Le, Cyrielle Rudaz, and Tatiana Budtova. 2014. Phase diagram, solubility limit and hydrodynamic properties of cellulose in binary solvents with ionic liquid. *Carbohydrate polymers* 105, 237–243. DOI: <https://doi.org/10.1016/j.carbpol.2014.01.085>.
- [28] Kim A. Le, Romain Sescousse, and Tatiana Budtova. 2012. Influence of water on cellulose-EMIMAc solution properties: a viscometric study. *Cellulose* 19, 1, 45–54. DOI: <https://doi.org/10.1007/s10570-011-9610-3>.
- [29] Katherine S. Lefroy, Brent S. Murray, and Michael E. Ries. 2021. Rheological and NMR Studies of Cellulose Dissolution in the Ionic Liquid BmimAc. *The journal of physical chemistry. B* 125, 29, 8205–8218. DOI: <https://doi.org/10.1021/acs.jpcc.1c02848>.

- [30] Hanbin Liu, Kenneth L. Sale, Bradley M. Holmes, Blake A. Simmons, and Seema Singh. 2010. Understanding the interactions of cellulose with ionic liquids: a molecular dynamics study. *The journal of physical chemistry. B* 114, 12, 4293–4301. DOI: <https://doi.org/10.1021/jp9117437>.
- [31] Hsiao-Chuan Liu and Matthew W. Urban. 2021. Optical coherence viscometry. *Applied physics letters* 118, 16, 164102. DOI: <https://doi.org/10.1063/5.0048608>.
- [32] Yi-Ying Ma, Ze-Long Lu, Yun-Zhu Xing, Wei-Shi Zheng, and Chun-Guang Liu. 2024. A fresh perspective on dissociation mechanism of cellulose in DMAc/LiCl system based on Li bond theory. *International journal of biological macromolecules* 268, Pt 1, 131729. DOI: <https://doi.org/10.1016/j.ijbiomac.2024.131729>.
- [33] Martin Alberto Masuelli. 2014. *Mark-Houwink Parameters for Aqueous-Soluble Polymers and Biopolymers at Various Temperatures*. Paper. Retrieved from.
- [34] Shurui Miao, Rob Atkin, and Gregory Warr. 2022. Design and applications of biocompatible choline amino acid ionic liquids. *Green Chem.* 24, 19, 7281–7304. DOI: <https://doi.org/10.1039/D2GC02282F>.
- [35] Michael Michael, Roger N. Ibbett, and Oliver W. Howarth. 2000. Interaction of cellulose with amine oxide solvents. *Cellulose* 7, 1, 21–33. DOI: <https://doi.org/10.1023/A:1009263606864>.
- [36] David L. Minnick, Raul A. Flores, Matthew R. DeStefano, and Aaron M. Scurto. 2016. Cellulose Solubility in Ionic Liquid Mixtures: Temperature, Cosolvent, and Antisolvent Effects. *The journal of physical chemistry. B* 120, 32, 7906–7919. DOI: <https://doi.org/10.1021/acs.jpcc.6b04309>.
- [37] N. Mohd, S. F. S. Draman, M. S. N. Salleh, and N. B. Yusof. 2017. Dissolution of cellulose in ionic liquid: A review. In . AIP Conference Proceedings. Author(s), 20035. DOI: <https://doi.org/10.1063/1.4975450>.
- [38] N. Terinte, R. Ibbett, K. Schuster. 2011. Overview on native cellulose and microcrystalline cellulose / Structure studied by x-ray diffraction (WAXD): Comparison between measurement techniques. *Lenzinger Berichte* 89, 2011, 118–131.
- [39] Ramakrishnan Parthasarathi, Kanagasabai Balamurugan, Jian Shi, Venkatesan Subramanian, Blake A. Simmons, and Seema Singh. 2015. Theoretical Insights into the Role of Water in the Dissolution of Cellulose Using IL/Water Mixed Solvent Systems. *The*

*journal of physical chemistry. B* 119, 45, 14339–14349. DOI:

<https://doi.org/10.1021/acs.jpcc.5b02680>.

- [40] André Pinkert, Kenneth N. Marsh, and Shusheng Pang. 2010. Reflections on the Solubility of Cellulose. *Ind. Eng. Chem. Res.* 49, 22, 11121–11130. DOI: <https://doi.org/10.1021/ie1006596>.
- [41] Antje Potthast, Thomas Rosenau, Richard Buchner, Thomas Röder, Gerald Ebner, Hartmut Bruglachner, Herbert Sixta, and Paul Kosma. 2002. The cellulose solvent system N,N-dimethylacetamide/lithium chloride revisited: the effect of water on physicochemical properties and chemical stability. *Cellulose* 9, 1, 41–53. DOI: <https://doi.org/10.1023/A:1015811712657>.
- [42] Jérémy Rebière, Maëlie Heuls, Patrice Castignolles, Marianne Gaborieau, Antoine Rouilly, Frédéric Violleau, and Vanessa Durrieu. 2016. Structural modifications of cellulose samples after dissolution into various solvent systems. *Analytical and bioanalytical chemistry* 408, 29, 8403–8414. DOI: <https://doi.org/10.1007/s00216-016-9958-1>.
- [43] T. Röder, B. Morgenstern, N. Schelosky, and O. Glatter. 2001. Solutions of cellulose in N,N-dimethylacetamide/lithium chloride studied by light scattering methods. *Polymer* 42, 16, 6765–6773. DOI: [https://doi.org/10.1016/S0032-3861\(01\)00170-7](https://doi.org/10.1016/S0032-3861(01)00170-7).
- [44] Cyrielle Rudaz and Tatiana Budtova. 2013. Rheological and hydrodynamic properties of cellulose acetate/ionic liquid solutions. *Carbohydrate polymers* 92, 2, 1966–1971. DOI: <https://doi.org/10.1016/j.carbpol.2012.11.066>.
- [45] Romain Sescousse, Kim A. Le, Michael E. Ries, and Tatiana Budtova. 2010. Viscosity of cellulose-imidazolium-based ionic liquid solutions. *The journal of physical chemistry. B* 114, 21, 7222–7228. DOI: <https://doi.org/10.1021/jp1024203>.
- [46] Sigma Aldrich Homepage. 2023. *Avicel PH-101 particle size 50um 9004-34-6* (August 2023). Retrieved August 22, 2023 from <https://www.sigmaaldrich.com/JP/en/product/sial/11365>.
- [47] Stephan Silbermann, Christian Weilach, Gerhard Kliba, Karin Fackler, and Antje Potthast. 2017. Improving molar mass analysis of cellulose samples with limited solubility. *Carbohydrate polymers* 178, 302–310. DOI: <https://doi.org/10.1016/j.carbpol.2017.09.031>.
- [48] L. H. Sperling. 2006. *Introduction to physical polymer science*. (4th ed.). Wiley, New York, Chichester.

- [49] David Steinbach, Andrea Kruse, Jörg Sauer, and Jonas Storz. 2020. Is Steam Explosion a Promising Pretreatment for Acid Hydrolysis of Lignocellulosic Biomass? *Processes* 8, 12, 1626. DOI: <https://doi.org/10.3390/pr8121626>.
- [50] Djalal Trache, M. H. Hussin, Caryn T. Hui Chuin, Sumiyyah Sabar, M. R. N. Fazita, Owolabi F. A. Taiwo, T. M. Hassan, and M. K. M. Haafiz. 2016. Microcrystalline cellulose: Isolation, characterization and bio-composites application-A review. *International journal of biological macromolecules* 93, Pt A, 789–804. DOI: <https://doi.org/10.1016/j.ijbiomac.2016.09.056>.
- [51] Huaizhong Xu, Tilman Bronner, Masaki Yamamoto, and Hideki Yamane. 2018. Regeneration of cellulose dissolved in ionic liquid using laser-heated melt-electrospinning. *Carbohydrate polymers* 201, 182–188. DOI: <https://doi.org/10.1016/j.carbpol.2018.08.062>.
- [52] Chao Zhang, Ruigang Liu, Junfeng Xiang, Hongliang Kang, Zhijing Liu, and Yong Huang. 2014. Dissolution mechanism of cellulose in N,N-dimethylacetamide/lithium chloride: revisiting through molecular interactions. *The journal of physical chemistry. B* 118, 31, 9507–9514. DOI: <https://doi.org/10.1021/jp506013c>.
- [53] Yuling Zhao, Xiaomin Liu, Jianji Wang, and Suojiang Zhang. 2013. Insight into the cosolvent effect of cellulose dissolution in imidazolium-based ionic liquid systems. *The journal of physical chemistry. B* 117, 30, 9042–9049. DOI: <https://doi.org/10.1021/jp4038039>.
- [54] Yan Zhou, Xiaocheng Zhang, Jinming Zhang, Yaohui Cheng, Jin Wu, Jian Yu, and Jun Zhang. 2021. Molecular weight characterization of cellulose using ionic liquids. *Polymer Testing* 93, 106985. DOI: <https://doi.org/10.1016/j.polymertesting.2020.106985>.

## 8 Appendix

### 8.1 Figures

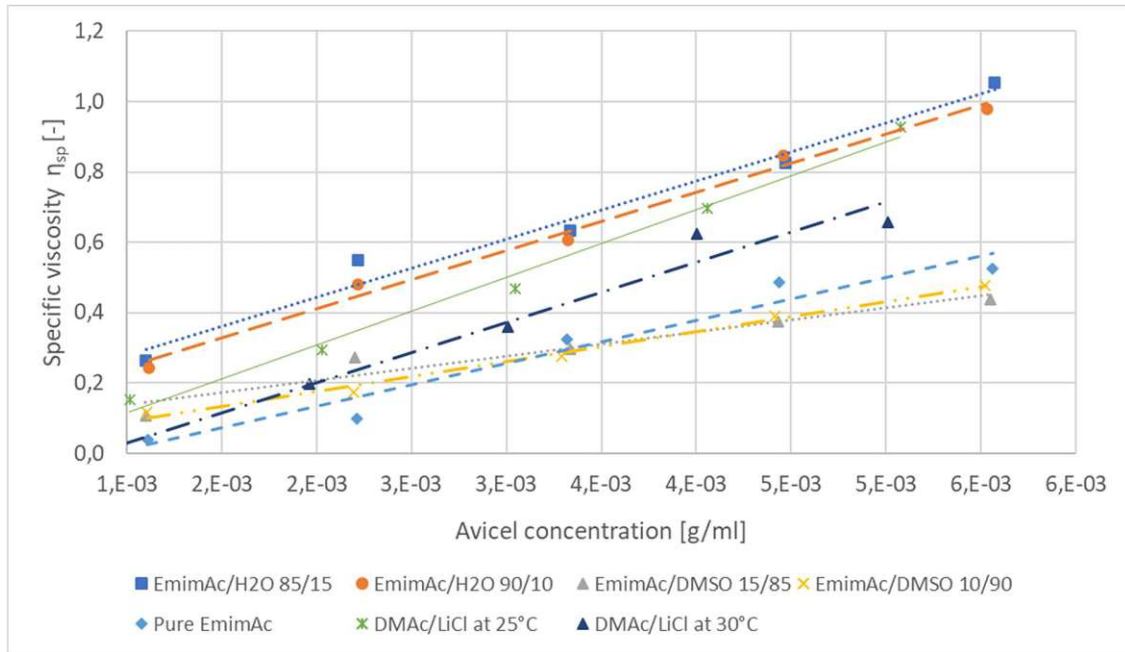


**Figure 8-1 Specific viscosities of EmimAc/H<sub>2</sub>O, EmimAc/DMSO, and DMAc/LiCl over Avicel concentration in the solution**

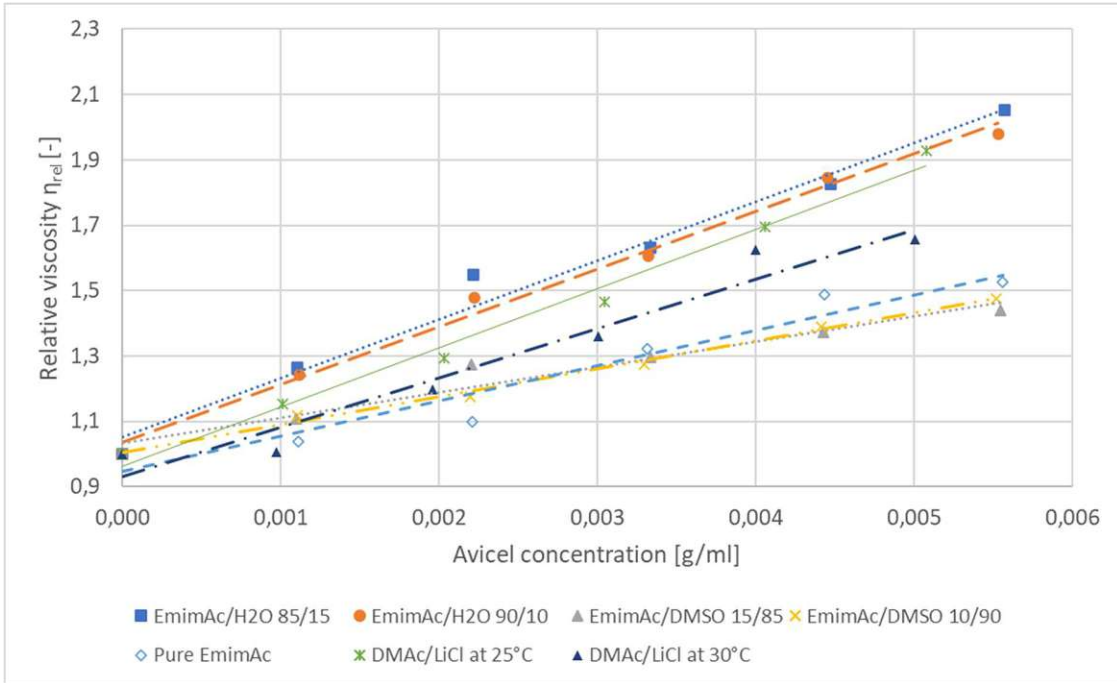


**Figure 8-2** Relative viscosity of EmimAc/H<sub>2</sub>O, EmimAc/DMSO, and DMAc/LiCl over Avicel concentration in the solution

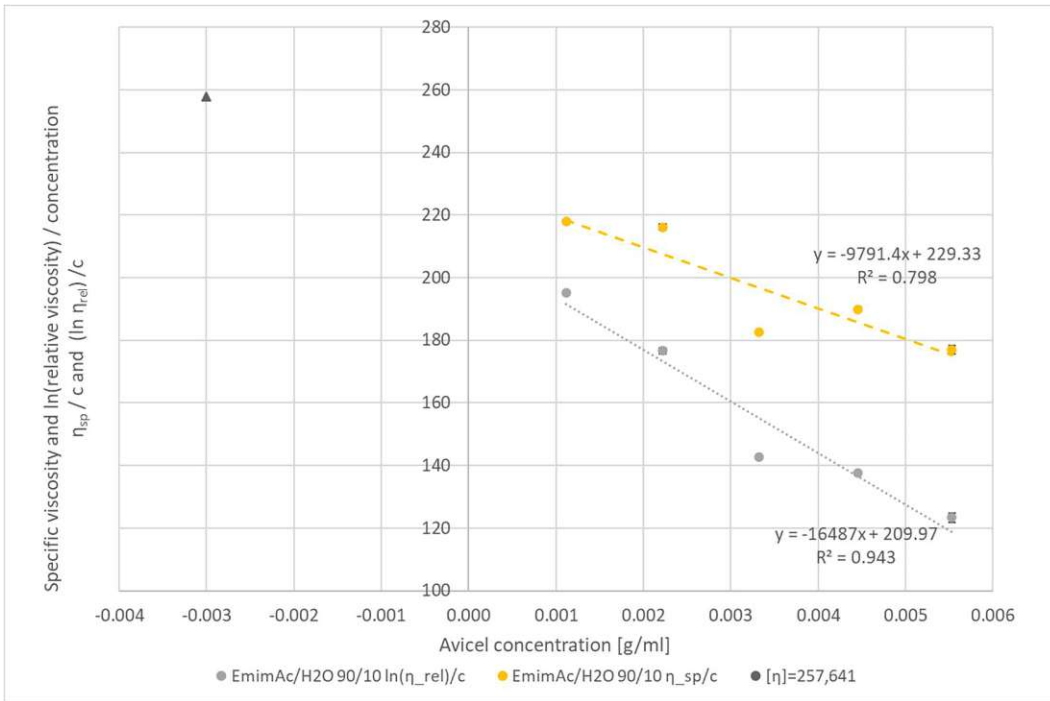


**Figure 8-3** Calculated intrinsic viscosity of EmimAc/H<sub>2</sub>O with ratio 90/10

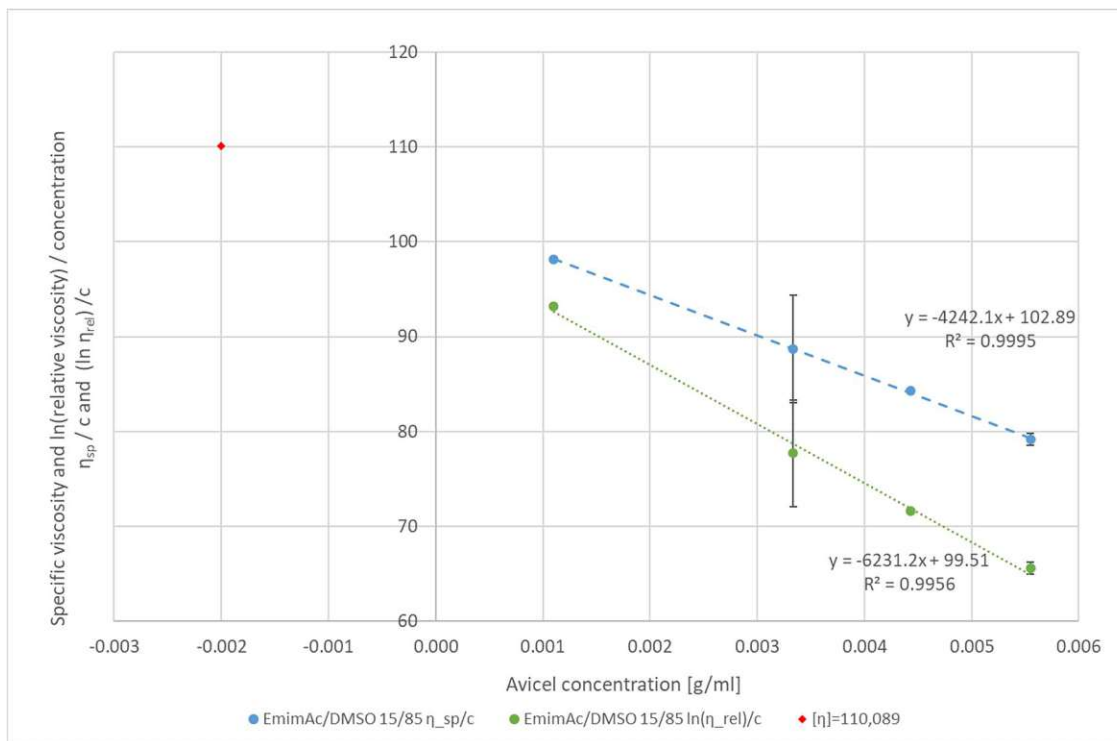


**Figure 8-4** Calculated intrinsic viscosity of EmimAc/DMSO with ratio 15/85

The standard deviation in Figure 8-4 for the 0.003 measured point is higher compared to the other results. Due to the high  $R^2$  of both lines, taking out this point does not change the result for  $[\eta]$  significantly. The 0.002 measured point was left out, due to an unrealistic result.

## 8.2 Calculation of heat flux Q for water/air – viscosity measurement

To calculate the heat flux Q, the heat transfer coefficient  $\lambda$  needs to be known for the system. The heat transfer coefficient depends on factors like the water's flow speed, the type of flow (laminar or turbulent), the surface geometry, and the specific properties of the water. Since the exact heat transfer coefficient is not available, I assume a typical value for water flowing in air under normal conditions. Heat transfer coefficients for water transferring heat to air usually range from 10 to 100  $\text{W}/\text{m}^2 \cdot \text{K}$  [3].

I assume a heat transfer coefficient of  $\lambda = 50 \text{ W}/\text{m}^2 \cdot \text{K}$ , as a middle value used for many standard applications.

The temperature difference is already known:  $T_{\text{water},1}=25^{\circ}\text{C}$ ,  $T_{\text{water},2}=30^{\circ}\text{C}$ ,  $T_{\text{air}}=22.5^{\circ}\text{C}$  (average room temperature during the experiments)

$$\Delta T_1=25^{\circ}\text{C}-22.5^{\circ}\text{C}=2.5^{\circ}\text{C} / \Delta T_2=30^{\circ}\text{C}-22.5^{\circ}\text{C}=7.5^{\circ}\text{C}$$

The heat flux  $Q$  is calculated using the following formula:

$Q=\lambda \cdot A \cdot \Delta T$ ,  $A$  is given by the description of the apparatus in 3.3, with a diameter of 35cm.

Substitute these into the formula:

The heat flux from the flowing water at  $25^{\circ}\text{C}$  to the surrounding air is 12 Watts.

The heat flux from the flowing water at  $25^{\circ}\text{C}$  to the surrounding air is 36 Watts.